Molecular characterization of nervous system organization in the hemichordate *Saccoglossus kowalevskii*

José M. Andrade Lopéz, Ariel M. Pani, Mike Wu, John Gerhart, Christopher J. Lowe

1) Hopkins Marine Station, Department of Biology, Stanford University, 120 Oceanview Blvd., Pacific Grove, CA 93950, United States
2) Departments of Biology and Cell Biology, University of Virginia, 90 Geldard Drive, Charlottesville, VA 22903
3) Department of Molecular and Cell Biology, University of California, 142 Life Sciences Addition #3200, Berkeley, CA 94720-3200

Abstract

Hemichordates are a key phylum for investigating the evolution of bilaterian nervous systems. As the closest chordate outgroup with a bilaterally symmetric adult body plan, hemichordates are particularly informative for exploring the origins of chordates and their centralized dorsal nervous system. Despite the importance of hemichordate neuroanatomy for testing hypotheses on deuterostome and chordate evolution, adult hemichordate nervous systems have not been comprehensively described using molecular techniques, and classic histological descriptions disagree on basic aspects of nervous system organization including the distribution of neurons in the body. A molecular description of hemichordate nervous system organization will be important for both anatomical comparisons and for attempts to understand how changes to ancient gene regulatory programs for ectodermal patterning relate to morphological evolution in deep time. Here, we describe the basic organization of the adult hemichordate *Saccoglossus kowalevskii* nervous system using immunofluorescence, *in situ* hybridization, and transgenic reporters to visualize neurons, neuropil, and key neuronal cell types. Consistent with previous descriptions, we found the *S. kowalevskii* nervous system consists of a pervasive nerve plexus that is concentrated in the anterior, along with nerve cords on both the dorsal and ventral sides. Neuronal cell types exhibited clear anteroposterior and dorsoventral regionalization in multiple areas of the body. We observed spatially demarcated expression patterns for many genes involved in synthesis or transport of neurotransmitters and neuropeptides but did not observe clear distinctions between putatively centralized and decentralized portions of the nervous system. In the trunk, there is a clear division of cell types between the dorsal and ventral cords suggesting differences in function. An extensive plexus concentrated in the anterior shows regionalized structure and is consistent with the proboscis base as a major site for information processing rather than the dorsal nerve cord. The absence of neural processes crossing the basement membrane into muscle and the presence of axonal varicosities suggest that volumetric transmission may play an important role in neural function. These data now facilitate more informed neural comparisons between hemichordates and other groups and contribute to broader debates on the origins and evolution of bilaterian nervous systems.

Introduction

The evolution and origins of animal nervous systems has been a topic of debate in comparative literature for over a century, particularly in reference to the origins of the chordate nervous system (Bateson, 1886; Garstang, 1894; Garstang, 1928; Geoffroy-St. Hilaire, 1822). With the emergence of molecular genetic data, the origins of central nervous systems (CNS) have been

a fascination in the field of evolution of development (Arendt and Nubler-Jung, 1996; De Robertis and Sasai, 1996; Denes et al., 2007; Hirth, 2010; Holland, 2015; Lowe et al., 2003; Martin-Duran et al., 2018). Classical comparative neurobiology has a rich and long history with broad phylogenetic sampling that was instrumental in developing many of the major hypotheses in neurobiology and nervous system evolution (Bullock and Horridge, 1965). The spectacular innovations in molecular neuroscience have given unprecedented insights into neural function (Luo, 2020). However, the focus of this work has been largely on biological models with highly centralized nervous systems and strong cephalization, particularly arthropods and vertebrates (Hejnol and Lowe, 2015). There have been fewer comprehensive molecular studies in phyla outside of these clades, particularly in animals with more sedentary lifestyles and less obvious centralization. Yet, for a broader understanding of nervous system evolution in metazoans, contemporary molecular data from these phyla is essential. This is now particularly pressing, as the generation of comparative developmental patterning data of regulatory genes, with key roles in CNS specification and patterning of arthropods and vertebrates, has now been investigated quite broadly phylogenetically, and by far outpaced parallel contemporary characterizations of neural cell type identity, and nervous system structure and function in the same representative species. Application of modern molecular tools of neurobiology to a wider range of species representing a broader sampling of neural systems is now essential, and not only test prevailing views on the evolution of the nervous system, but also provide novel opportunities to investigate neural circuit evolution.

Hemichordates are a group of marine invertebrates with sedentary adult life histories that have long been of comparative interest particularly in relation to chordate evolution (Kaul-Strehlow and Röttinger, 2015; Lowe, 2021; Tassia et al., 2016). Hemichordates were originally grouped within chordates due to proposed morphological affinities with chordates (Bateson, 1885). A close phylogenetic relationship with echinoderms based on larval morphology were recognized as early as the late 1800s (Metschnikoff, 1881), and all molecular studies have robustly grouped hemichordates as the sister group of echinoderms within the deuterostomes (Bromham and Degnan, 1999; Cameron et al., 2000; Cannon et al., 2014; Furlong and Holland, 2002). Hemichordates are divided into two major lineages; Enteropneusta and Pterobranchia. Enteropneusta are free-living worms that mainly live in burrows feeding by filter feeding or by particle ingestion, whereas Pterobranchs are small, largely colonial animals that have received far less research attention, due to their scarcity and small size (Sato et al., 2008; Tassia et al., 2016).

The earliest descriptions of the nervous system of enteropneusts using classical staining methods began in the late 1800s (Bateson, 1886; Kowalevsky, 1866; Spengel, 1877, 1903) and continued sporadically in the early to mid 1900s (Bullock, 1940, 1944; Bullock, 1945; Dawydoff, 1948; Hess, 1937; Knight-Jones, 1952). Only a few studies have used electron microscopy for more detailed structural observations (Dilly, 1969; Dilly et al., 1970; Kaul and Stach, 2010; Kaul-Strehlow and Stach, 2013). The enteropneust nervous system is largely intraepidermal with a basiepithelial plexus throughout the animal, but more prominent anteriorly in the proboscis and collar, and thickest at the base of the proboscis and proboscis stem (Figure 1). There are two cords, one ventral that is basiepidermal, extending from the posterior collar to the posterior of the trunk, and dorsal cord that extends along the entire extent of the dorsal midline. From the anus to the collar, this dorsal cord is superficial and basiepidermal, but the cord is internalized in the collar into a subepidermal cord, which in some species resembles vertebrate neural tube (Bateson, 1886; Kaul and Stach, 2010; Luttrell et al., 2012). At its most anterior extent, the collar cord emerges at the proboscis stem and continues as a superficial cord along the length of the

proboscis. The two cords are connected by a nerve ring in the posterior collar. Classical studies of hemichordate enteropneust nervous systems have come to contrasting conclusions on the most basic organizational principles of their structure and function. Some studies focused on the importance of the two cords, dorsal and ventral, acting as potential integration centers and concluded that hemichordates possess a CNS (Bateson, 1886; Hess, 1937; Morgan, 1894), whereas others have focused on the broadly distributed epithelial plexus with dorsal and ventral cords acting as conduction tracts instead of integration centers (Bullock, 1940; Bullock, 1945; Knight-Jones, 1952). From work in separate species, Bateson and Morgan concluded that the enteropneust collar cord, an intraepidermal cord, was homologous to the dorsal cord of chordates (Bateson, 1886; Morgan, 1894) because of the striking similarities to the subepidermal hollow cord, that in some species forms by a morphological process that strongly resembles vertebrate neurulation. Later studies in the 1930s-50s hypothesize that the dorsal and ventral cord were conduction tracts that lack neural cell bodies (Bullock 1945, Knight-Jones 1952). Bullock believed that the hemichordate nervous system more closely resembled the nerve net of cnidarians (Bullock 1945) whereas Knight-Jones alternatively proposed that the collar cord may be homologous to the neural tube in chordates but had since been secondarily simplified and is now largely a through tract rather than an integrative center (Knight-Jones 1952). More recent studies based on comparative morphology have added support to the hypothesis of homology between the hemichordate collar cord and the chordate dorsal cord (Kaul and Stach, 2010; Luttrell et al., 2012)

Recent interest in bilaterian neural system evolution has been driven by body patterning comparisons and the remarkable similarities between the development of central nervous systems of distantly related nervous systems (Arendt and Nubler-Jung, 1994; De Robertis, 2008; De Robertis and Sasai, 1996; Hirth, 2010; Hirth and Reichert, 1999; Lichtneckert and Reichert, 2005). Most molecular insights into hemichordate neural development have been inferential, using patterning genes rather than genes with roles in neural cell type differentiation (Aronowicz and Lowe, 2006; Darras et al., 2018; Gonzalez et al., 2017; Lowe et al., 2006; Lowe et al., 2003; Pani et al., 2012; Yao et al., 2016). However, some studies have focused specifically on genes with established roles in neural specification and differentiation, or cross-reactive antibodies for neural epitopes (Cunningham and Casey, 2014; Kaul-Strehlow et al., 2015; Lowe et al., 2003; Miyamoto et al., 2010; Nomaksteinsky et al., 2009). These studies have used pan-neural markers, like *elav* and synaptotagmin, and enzymes involved in neurotransmitter synthesis to study the hemichordate nervous system. Although limited, these studies have continued to show evidence of a broad plexus, but again have come to contrasting conclusions about the nature of the enteropneust nervous system. There is still no comprehensive study of neural subtypes and their distribution in hemichordates, nor a clear picture of the morphology for different cell types or structure of the neural plexus and cords.

Speculation on the organization of the enteropneust nervous system was reignited with the studies on the expression of gene regulatory networks (GRN) with conserved roles in patterning the CNS of many model species during the early development of *S. kowalevskii*. The GRN for anterior-posterior CNS patterning that is well conserved between several protostomes groups and chordates is also conserved in hemichordates along the AP axis even though the nervous systems they specify are anatomically very different (Darras et al., 2018; Gonzalez et al., 2017; Kaul-Strehlow et al., 2017; Lowe et al., 2003; Pani et al., 2012; Yao et al., 2016). These genes are expressed in circular bands around the ectoderm in hemichordates, rather than expressed in a tight domain associated with either the dorsal or ventral cords, unlike in vertebrates where they are most prominently expressed in the developing brain and nerve cord (Pani et al., 2012).

The neural structures specified by this conserved network have evolved independently and represent highly divergent structures despite the tight conservation in their gene regulatory networks. Therefore, it remains an open question as to whether there are some elements of neural conservation despite the overt differences in the organizational elements of their respective nervous systems. It also remains a possibility that there are neural cell type homologies under conserved positional regulation between vertebrates and hemichordates. A closer examination of the molecular neurobiology of hemichordates and the potential link to conserved suites of regulatory genes will contribute to the discussion about how molecular genetic data can be used to reconstruct ancestral neural architectures.

Here we characterize the expression of multiple neural markers using *in situ* hybridization, and immunohistochemistry to characterize the location and degree of specialization of the nervous system along both the AP and DV axes, and the extent and structure of the neural plexus. We also used mosaic transgenic approaches to determine cellular morphologies and projection patterns of neural subpopulations. Our data provides the first comprehensive description of an adult hemichordate nervous system using molecular methods, which will facilitate comparisons to other bilaterians.

Results

Extent and regionalization of neural markers along the A/P and D/V axes

Many classical studies of enteropneust nervous systems used histological techniques, such as Golgi stains, that generally work well in animals with a clearly defined CNS where neurons are segregated from the general epithelium. However, these methods may not unambiguously distinguish neural from epidermal cells in animals, like enteropneusts, where the nervous system is intraepidermal. Consequently, the number, diversity, and distribution of neurons along the A/P and D/V axes of the adult animals has been a source of controversy (Bullock, 1945). We examined expression of a wide range of neural/neurosecretory markers in post-hatching juvenile and fully grown adult animals, using *in situ* hybridization. Previous studies have demonstrated that neurons are specified across broad domains during embryogenesis, and nerve cords are first apparent during late stages of embryonic development (Cunningham and Casey, 2014; Kaul-Strehlow et al., 2015). Our study focused on post-hatching juveniles as the animal possesses almost all the adult characteristics but are smaller and more amenable to whole-mount microscopy. This initial part of our study establishes a more accurate assessment of neural cell body number, the extent of neural subtypes, and how they are distributed along the major organizational axes.

***Elav* expression in the *S. kowalevskii* nervous system:** *Embryonic lethal abnormal visual system (elav*) is a conserved RNA binding protein, first discovered in *Drosophila melanogaste* that has been used in many organisms as a putative pan-neuronal marker (Cunningham and Casey, 2014; Robinow et al., 1988; Robinow and White, 1988). However, expression of *elav* has been reported in other cell types, and not in all neurons (Pham and Hobert, 2019; Sanfilippo et al., 2016), so caution should be used when only using this marker to fully represent neural complements in developing models. We first sought to identify the distribution of *elav*+ cells in juveniles and adult tissue by *in situ* hybridization, extending the scope of previous studies at earlier developmental stages (Cunningham and Casey, 2014; Lowe et al., 2003). The use of this gene has previously shown the tight association of *elav* expression with the forming cords on

the midline and broadly in the proboscis ectoderm (Cunningham and Casey, 2014; Kaul-Strehlow et al., 2017; Lowe et al., 2003; Nomaksteinsky et al., 2009), but with few cells outside of the cords, posterior to the collar.

We first examined *elav* expression in adult *S. kowalevskii* through a comprehensive series of adult sections in both transverse and sagittal planes (Figure 1A). The transverse plane at mid-proboscis shows circumferential *elav* expression in the most basal layer of the epithelium, and more marked staining along the dorsal midline (Figure 1B). The cross section at the proboscis base has a thicker band of expression, supporting previous observations of neural condensation in this region (Nomaksteinsky et al., 2009)(Figure 1C). At the anterior collar, we detected expression of *elav* throughout the pharyngeal epithelium (Figure 1D-G) and evidence of the anterior collar nerve ring in the ectoderm (Figure 1D). In addition, there is a prominent layer of *elav* expression dorsal to processes in the dorsal cord, representing the soma of that runs the length of the collar as an internal collar cord (Figure 1D-I). Expression in the general ectoderm of collar and trunk is sparse, as described previously in *Ptychodera flava* (Nomaksteinsky et al., 2009) but cells are detected in the epithelium in the posterior collar and trunk (Figure 1H-J). Sagittal sections show a gradient of *elav* expression in the proboscis increasing towards the base, an anterior collar ring (ACR) and posterior collar ring, and expression in the pharyngeal endoderm (Figure 1K,L,M). The middle sagittal section clearly shows the trajectory of the collar cord (Figure 1L). The enteric nervous system is also visible in the endoderm with dispersed *elav+* cells in the gut (Figure 1M). At late juvenile stage, characterized by the presence of 3-gill slits (3GS), *elav+* cells are distributed similarly to their distribution in adults; throughout the proboscis ectoderm, with a concentration at the proboscis base, and also along the entire dorsal and ventral cords (Figure 1N). The proboscis dorsal cord is also visible and extends anteriorly from the collar cord (Figure 1O). The similarities between adult and late juvenile suggests that the juvenile is a reasonable approximation for basic organization of adult neural characters.

Given the comparative interest in hemichordate trunk nerve cords and distribution of neurons in the skin, we examined *elav* expression closely in adults using whole mount *in situ* hybridization to visualize cell populations that may be difficult to observe in tissue sections. In the ventral cord, expression of *elav* is broadly expressed in a wide band of ectoderm. Rows of clustered cells are present in columns, perpendicular to the cord, along ridges of the epithelium (Figure 1P). On the dorsal side, a thin line of *elav+* cells is present along the length of the proboscis (Figure 1Q), along with the broad expression shown in sections (Figure 1B,C). Expression is also detected in two narrow rows of cells that flank the dorsal midline along the length of the trunk (Figure 1R,S). In the trunk, the *elav+* domain is markedly narrower on the dorsal side than the ventral side. In the posterior trunk, *elav+* cells are also distributed in clusters of cells throughout the epithelium, possibly associated with the calcified granules embedded in this region (Figure 1S).

Regionalization of neural subtypes.

Expression of neurotransmitter and neuropeptide biosynthesis and transport markers: While general neural markers like *elav* give a broad picture of the localization of neurons, they do not give any insights into the extent of neural diversity, or how neural subpopulations are organized. Expression of genes involved in the biosynthesis and transport of neurotransmitters and neuropeptides provides information about the extent of neural differentiation, and how organized their expression domains are along organizational axes. We performed *in situ* hybridization for components of neurotransmitter and neuropeptide signaling, including proteins

involved in their synthesis and transport in juvenile, both at the 1 gill-slit (1GS) and 3GS stage, and in some cases, in adult tissue.

Neurotransmitter synthesis and transport.
Neurotransmitters are small molecules used by neurons as chemical messengers to communicate across cells. They can transmit an excitatory or inhibitory signal synaptically, or modulate neuronal activity non-synaptically using biogenic amines (or monoamines) and amino acids. Genes involved in neurotransmitter synthesis and transport are often highly regionalized in the nervous systems of model bilaterian species.

Monoamines: In *Saccoglossus* juveniles, the location of catecholaminergic neurons is revealed by the expression of *tyrosine hydroxylase* (*TH*) in scattered cells at several different domains in the ectoderm. Early developmental stages were examined previously (Cunningham and Casey, 2014). In early juveniles, shortly after hatching *TH* expression is restricted to isolated cells in the anterior proboscis ectoderm, and broadly in the anterior trunk, wrapping around the forming first gill slit (Cunningham and Casey, 2014; Pani et al., 2012). This pattern continues in the later juvenile stages before hatching with the addition of a thin circumferential line close to the base of the proboscis (Figure 2A). The expression around the gill slits is far more diffuse and extensive than the more cell type specific staining in the proboscis and collar (Figure 2A,B,D). In post hatching juveniles, an additional prominent band of cells forms at the anterior tip of the collar (Figure 2B). The same general expression domains persist through to adults, but with an expanded anterior proboscis domain (Figure 2C'), and additional isolated cells in the collar, with a strong anterior collar domain, and row of cells at the base of the proboscis (Figure 2C''). To specifically identify dopaminergic neurons, we examined the expression of *dopamine transporter* (*DAT*). In juveniles, *DAT* is co-expressed in many of the same cells in the juveniles (Figure 2D); in the anterior proboscis (Figure 2D') and in anterior collar (Figure 2D''). *TH+* cells at the base of the proboscis were conspicuously missing *DAT* co-expression raising the possibility they may represent other types of catecholaminergic neurons. However, in older juveniles, *DAT* is expressed in this region and supports the DA neural identity (Figure 2E).
The distribution of *tryptophan hydroxylase* (*TPH*), marking serotonergic neurons, was previously reported at earlier developmental stages (Cunningham and Casey, 2014). Here we confirm isolated cellular expression in a broad circumferential domain in the proboscis ectoderm shortly after hatching (Figure 2F). Histamine is synthesized from histidine by *histidine decarboxylase* (*HDC*) and is a marker for histaminergic neurons (Watanabe et al., 1984). In juveniles, expression of *HDC* is sharply defined in the posterior proboscis in a broad ectodermal domain rather than punctate individual cells, which may indicate a broader ectodermal distribution of histamine rather than specifically neuronal (Figure 2G). Additionally, more punctate staining is detected in the ventral ectoderm narrowing to the ventral cord at later stages, and scattered large cells along the dorsal cord in the trunk, which refine to a more posterior territory at later stages (Figure 2G,H).

Amino acid neurotransmitters
Two major amino acid neurotransmitters are glutamate and GABA. Glutamate is a major excitatory neurotransmitter across bilaterians and non-bilaterians (Antzoulatos and Byrne, 2004; Danbolt, 2001; Fonnum, 1984; Greer et al., 2017; Nistri and Constanti, 1979) . GABA has a conserved role in bilaterians as an inhibitory neurotransmitter in both the CNS and PNS in invertebrates and vertebrates (Gerschenfeld, 1973; Jackson et al., 1990; McIntire et al., 1993; Miller, 2019; Mueller et al., 2006; Nistri and Constanti, 1979; Roberts et al., 1976). Expression of *glutamate decarboxylase* (*GAD*) has been used to characterize the distribution of GABA–

producing neurons (Roberts and Kuriyama, 1968) along with the GABA transporter *VGAT* (Kinjo et al., 2013), whereas glutamatergic neurons have been identified by the expression of its transporter, *VGluT*.

In *Saccoglossus* juveniles, *VGluT* is detected in isolated cells in the ectoderm of the proboscis and anterior collar (Figure 2I). In the trunk, it is detected in two rows of cells on either side of the dorsal midline along the trunk, posterior to the collar (Figure 2I, inset) at early juvenile stage and in scattered cells broadly in the posterior. In 3GS juveniles, expression in the proboscis remains broadly dispersed, and there are two circumferential lines of cells in both the anterior and posterior collar (Figure 2J'). Expression extends down the trunk, again along the dorsal midline in a broad territory, wider than the extent of the cord defined by the expression of *elav* (Fig1N,O,R), but also dispersed in the general ectoderm (Figure 2J''). *GAD* is expressed in scattered ectodermal cells in defined domains throughout different developmental stages. In early juveniles it is expressed throughout the entire proboscis, but most prominently in the anterior tip and at the proboscis base (Figure 2K). At later juvenile stages, the anterior and posterior ectodermal, circumferential domains become more prominent, and a sharp, narrow band of expression at the very anterior lip of the collar is detected in a circumferential domain. At these later stages, expression is now detected in isolated cells in the posterior region of the pharynx and in scattered cells in the dorsal cord of the trunk (Figure 2L). The juvenile expression is consistent with the patterns found in adult animals: the whole mount *in situ* hybridization of adult *GAD* expression reveals a dense anterior expression domain that becomes increasingly diffuse down towards the proboscis base (Figure 2M'). There is a pronounced ring of cells at the proboscis base that is contiguous except dorsally where the ring terminates with a pair of prominent cell clusters on either side of the dorsal midline (Figure 2M''). The anterior lip of the collar has a similar ring in isolated cells (Figure 2M''). The distribution of the GABA transporter *VGAT* in early juveniles shows very similar expression domains to *GAD* at early juvenile stages, with strong expression at the base of the proboscis and cells scattered throughout the ectoderm (Figure 2N). However, we do not observe expression in the anterior proboscis where *GAD* is localized at either early or late juvenile stage.

<u>Neuropeptides</u>

Neuropeptides are the largest and most diverse signaling molecules ranging from 3-40+ amino acids that are involved in neurotransmission, neuromodulation or hormonal functions (Burbach, 2011; van den Pol, 2012). Most neuropeptides signal through G protein-coupled receptors (GPCRs) to modulate downstream activities (Hewes and Taghert, 2001; Jekely, 2013). Previous studies have identified an array of conserved neuropeptides and their GPCR receptors in *S. kowalevskii* (Elphick, 2010; Elphick and Mirabeau, 2014; Jekely, 2013; Krishnan et al., 2013; Mirabeau and Joly, 2013). Two general neuropeptide synthesis enzymes are Prohormone convertase 2 (PC2) and glutaminyl-peptide cyclotransferase (GPC), which catalyzes the posttranslational modification of the N-terminal glutamine of peptide hormones (Busby et al., 1987; Fischer and Spiess, 1987; Rouille et al., 1995; Seidah et al., 1999; Zhang et al., 2010). By looking at the expression of these two general neuropeptide synthesis markers, we can determine which regions of the nervous system are actively producing the diverse array of neuropeptides identified in *S. kowalevskii.* As is expected, expression of these enzymes exhibit generally overlapping localization in both early and late juveniles (Figure 2O-P'). In early juveniles, PC2 is broadly expressed in the proboscis, but strongest at the base. It has a tight ring of expression in the anterior collar, in the collar/dorsal cord, and in the developing ventral cord (Figure 2O). Expression in the later juvenile is strongest at the base of the proboscis, anterior collar ring, and anterior ventral cord, whereas expression in the anterior proboscis and

dorsal cord becomes less prominent (Figure 2O'). GPC expression is more dorsally localized at the proboscis base with more punctate expression in the ventral ectoderm (Figure 2P,P') whereas PC2 expression is more uniform in a thick band around at the proboscis base (Figure 2O,O'). We also observed expression in the more posterior regions of the dorsal and ventral cords. Together, these enzymes are expressed at the five major regions of the ectoderm: anterior proboscis, posterior proboscis, anterior collar, dorsal cord, and the ventral cord and overlap in their expression domains in the proboscis and collar with several of the neurotransmitter systems.

A wide range of neuropeptides have been identified in *S. kowalevskii* (Elphick, 2010; Elphick and Mirabeau, 2014; Jekely, 2013; Krishnan et al., 2013; Mirabeau and Joly, 2013), and we investigated the expression of a small subset of these. A major group of neuropeptides are the RFamides, which have the conserved C-terminal RFamide. There are hundreds of RFamides that have been described across bilaterians, and each is involved in diverse roles ranging from osmoregulation, muscle contractions, reproduction, feeding and digestion (Elphick and Mirabeau, 2014; Jekely, 2013; Mirabeau and Joly, 2013; Walker et al., 2009). The original RFamide, FRMRamide, was identified from the ganglia of a mollusk, *Macrocallista nimbosa*, and was later characterized for its role as a caridioexcitatory neuropeptide (Price & Greenberg 1977).

S. kowalevskii also contains several RFamide-class neuropeptides. NNFG is expressed in the proboscis ectoderm in two main domains; the most prominent is in a strong, circumferential, horseshoe-shaped band with expression absent in the most dorsal territory, close to the base of the proboscis (Figure 2Q,Q'). The second domain is defined by scattered individual cells visible in the entire anterior half of the proboscis ectoderm, all the way to the anterior tip. WMRFamide expression appears in a circular band at the proboscis base, though WMRFamide is expressed more posteriorly than the FMRFamide band as two dorsal spots (Figure 2R,R'). The conserved bilaterian neuropeptide luqin (Luq), subsequently lost in the chordate lineage (Elphick and Mirabeau, 2014), is another RFamide-related neuropeptide. Comparative studies across bilaterians suggest a shared role in chemosensory and locomotion control through flask shaped, ciliated RFamide neurons (Tessmar-Raible et al., 2007). Luq is initially expressed in the posterior proboscis and anterior collar at the 1GS stage but expression is later detected at the anterior and posterior proboscis, anterior collar, both the dorsal and ventral cord, and the ventral cord extends towards the post anal tail in 3GS juveniles (Figure 2S,S').

Other neuropeptides include VIamide (VIG), achatin, cholecystokinin, and orexin. The latter 3 peptides are all conserved within bilaterians (Elphick and Mirabeau, 2014; Elphick et al., 2018; Jekely, 2013). VIG is characterized by an anterior/dorsal domain of expression 3GS juveniles, with isolated cells revealed along the dorsal midline from the anterior tip to about half way down the proboscis. The expression is clear enough that the flask-shaped morphology of the cells is apparent (Figure 2T). Achatin shows restricted expression in large isolated cells distributed in the anterior proboscis (Figure 2U,U'). Cholecystokinin (CCK) is a gastrointestinal hormone peptide that has an ancient role in regulating feeding (Tinoco et al., 2021). CCK is expressed in the proboscis base in early juveniles (Figure 2V) and later has broader expression in the pharynx endoderm and ventral trunk ectoderm in late juveniles (Figure 2V'). Orexin is another bilaterian-conserved neuropeptide broadly expressed throughout the epithelium in 1GS and 3GS juveniles, with minimal expression around the collar (Figure 2W, W').

Unlike neurotransmitters, which preferentially exhibit anterior expression, neuropeptides show more extensive posterior expression along the ventral and dorsal cords. Expression data for neurotransmitter and neuropeptide synthesis and transport markers suggests that *S. kowalevskii* has a strongly regionalized nervous system, with an increased neural cell type diversity in 5 main territories; the anterior proboscis, posterior proboscis, anterior collar, dorsal cord, ventral cord; but most prominently, the dorsal proboscis base.

Plexus and neural cord organization

In the previous section we described the expression of many important genes involved in neural function by *in situ* hybridization. These data provide useful information about specialization and location of neuronal cell bodies, but tells us little about neural morphology, neurite and axonal projections, and the general structure of the nervous system. In order to begin to investigate nervous system structure and function, we performed immunohistochemistry for a monoclonal antibody (1E11) to the pan-neural marker synaptotagmin, which was developed from the radial nerve extract of asteroid, *Asterina pectinifera* (Nakajima et al., 2004b), to visualize cell morphology and neurite projections in juveniles and adults (Figure 3A). Previous comparative work has validated the cross reactivity of this antibody localizing to neurons in other ambulacrarian taxa; broadly in echinoderms and in another species of hemichordate (Byrne et al., 2007; Nakajima et al., 2004a).

Whole mount immunohistochemistry of late juveniles at the 3GS stage revealed a complex and structured nervous system with a dense basiepithelial nerve plexus throughout the proboscis, but thicker at the base (Figure 3A). Neurites and axons are well-labelled, but cell bodies had weak signal (Figure 3B). The plexus is also very prominent in the collar ectoderm, but much less in the trunk. An endodermal plexus is visible throughout the pharynx. The subepidermal collar cord is clearly visible extending from the thick plexus at the dorsal posterior ectoderm of the proboscis into the superficial dorsal cord, which begins in the posterior collar and runs the length of the trunk terminating at the anus. The wider superficial ventral cord begins at the posterior collar/anterior trunk boundary and extends posteriorly throughout the entire ventral midline of the animal.

We further utilized 1E11 to determine the structure of the nervous system in adults. As many of the neural cell type markers exhibit localized domains of expression in the proboscis, we first investigated 1E11 expression at this site. We examined the plexus in this territory by peeling off sections of ectoderm from the underlying proboscis mesoderm in fixed adults and carrying out whole mount immunohistochemistry on these tissue fragments (Figure 3C). In the general proboscis ectoderm, we observe a well-organized plexus with parallel bundles of processes running along the AP axis, with regularly spaced connectors projecting laterally between the bundles (Figure 3D). This organization is remarkably similar to the drawings of Knight-Jones (1952). The dorsal superficial cord is visible as a thickening of this plexus (Figure 3E). The neurite bundles projecting along the AP axis observed in the mid proboscis exhibit a striking transition in plexus structure: a complex architecture of thicker neurite bundles forming a series of layered, interconnected tracks. This can be clearly observed in Figure 3D where the flat mount of the ectoderm shows the parallel projections on the left of the panel projecting into the complex plexus at the proboscis base at the right of the panel. A z-stack of this territory more clearly shows the structure of the plexus (Supplementary Movie 1). Higher magnification shows the complex architecture of this territory (Figure 3F,G). The structure of this domain is very

reminiscent of the anterior territory of the plexus structure in the acoel *Hofstenia miamia* (Hulett et al., 2020) and the holes in the plexus may represent extensions from epithelial cells that attach to the basement membrane as reported from early EM studies (Dilly, 1969). Moving posteriorly into the collar, we observed a similar, structured plexus to the proboscis base, but with less densely packed tracts (Figure 3H). A z-stack (Supplemental Movie 2) in this region again clearly shows the structured nature of this plexus. Further posterior in the trunk, the plexus is less extensive than in the proboscis or collar, with the dorsal and ventral cords being the most prominent features representing condensations of the plexus along both midlines (Figure 3I).

The results from 1E11 reveal many general aspects of the distribution and organization of the neural plexus, but little resolution of individual neurites. We used injection of lipophilic dye (DiI) into adult fixed tissue in the mid proboscis to look more closely at the morphology and directionality of neurite projections. Individual neurites extend from the injection site in all directions, but with prominent neurite bundles projecting along an AP axis, matching what was observed with the IE11 antibody (Figure 3J,K). The plexus is clearly structured, with the imaging stacks showing different projection patterns according to the position along the apico/basal axis in the plexus. Lower volume injections of DiI imaged at higher magnification reveal many neurites with regular puncta along their length (Figure 3L,M). As these swellings may represent fixation artifacts, we utilized a live neural stain, NeuO, a membrane-permeable fluorescent probe (Er et al., 2015). We observe similarly labeled neurites/axons in the trunk revealing regularly spaced boutons along the neurites/axons (Figure 3N). The similar structures detected along the processes using both fixed (DiI) and live (NeuO) tissue suggest these structures may represent either *en passant* synapses (de Castro, 1950), or varicosities involved in volumetric release (Nieuwenhuys, 2000).

Morphology and projection of neural subtypes

Our *in situ* hybridization data for neurotransmitter and neuropeptide synthesis and transport markers clearly demonstrates that *S. kowalevskii* has strong regional specialization of its nervous system, and also revealed the location of cell bodies characterized by specific neurotransmitters and neuropeptides. However, these data provide no information about the directionality or length of projections, and *in situ* hybridization data rarely provides information about cellular morphology. We used two different methods to investigate details of neural subtype morphology and projections; cross reactive antisera to neurotransmitters and neural transgenics.

Cross reactive antisera:
<u>Serotonergic neurons</u>: We used an antibody raised to 5-HT to label serotonergic neurons in 3GS stage *S. kowalevskii* (Figure 4A). Previous work using this antibody has already investigated the distribution of the serotonergic nervous system in early developmental stages, in juveniles and limited sections in adults, and our data confirms expression and extends sampling of these studies (Brown et al., 2008; Cunningham and Casey, 2014; Kaul-Strehlow et al., 2015). Figure 4 shows the distribution of the serotonergic nervous system in juveniles and adults. In juveniles, the serotonergic nervous system is composed of primarily receptor, flask-shaped bipolar neurons broadly dispersed in the proboscis ectoderm and collar, but more sparsely in the trunk. In the proboscis, while staining is broadly scattered, there are no cell bodies detected in either the most apical ectoderm or at the base of the proboscis (Figure 4A,C). All neurons project into the underlying neural plexus, although it is not possible to trace

the full length of individual axons due to large numbers of projections in the plexus. However, proboscis neurons appear to generally project posteriorly, based on the orientation of the axon close to the cell body. In the collar, cell bodies are organized into three rings, two at the anterior and one at the mid collar (Figure 4A,D). These neurons also have a single dendrite and sensory cilium projecting out of the epithelium, and a single axon projecting basally into the neural plexus. There are positional differences in cell body location within the epithelium; some cell bodies are located basally and others more apically (Figure 4B). In the collar and proboscis, we see no dorsoventral differences in the distribution of cell bodies, however, cell bodies in the trunk are positioned on the dorsal side, mostly lateral to the dorsal cord but generally project ventrally into the ventral cord (Figure 4E). In the anterior part of the trunk, there are also cell bodies scattered in the ectoderm more laterally around the gill slits (Figure 4A). A z-stack of the serotonergic nervous system in this region again clearly shows the structured nature of this plexus, as well as dorsal sensory cells projecting laterally along the trunk towards the ventral cord (Supplementary Movie 2).

We further extended our analysis into adult animals. Whole mount immunohistochemistry in adults show a far more extensive serotonergic population than in juveniles but generally confirm a similar expression pattern established in juveniles. Figure 4F shows a view of the mid-proboscis, showing broad distribution cell bodies projecting into the underlying epithelium, with projections in all directions, but most projecting posteriorly, similar to the organization revealed from 1E11 (Figure 3E). The base of the proboscis (the same specimen as Figure 3D,E) double labelled for both 1E11 and 5HT (Figure 4G,H) reveals that serotonergic axons form a subset of the complex network of bundles. The morphology of the neurites shows swellings along the length of the processes similar to what we demonstrated with DiI labelling. In the collar (Figure 4I), staining is absent in the anterior lip, but just posterior there is a ring of expression in the ectoderm, and broad ectodermal labelling throughout the collar ectoderm. Cell bodies are more broadly dispersed throughout the collar epithelium, rather than in discrete rings as in 3GS juveniles. Note that these findings contrast with the lack of neural staining from *elav* in this region (Figure 1). In the posterior trunk, the epithelium is ruffled, and we observed patches of cell bodies in the lateral body wall, and an extensive, but thin, plexus throughout the trunk epithelium (Figure 4J).

We next investigated the labelling of the serotonergic neurons in representative cross sections along the adult body, counterstained with phalloidin (Figure 4K). In the posterior proboscis, we observe clear dorsoventral asymmetry in plexus thickness, with the dorsal region thicker than the ventral territory, and with cell bodies distributed more ventrally in this plane of section (Figure 4L). In the mid-collar (Figure 4M) the neural plexus is extensive in both the ectoderm and the endoderm but is thinner than the proboscis plexus (Figure 4L). The dorsal cord is clearly visible and shown in higher magnification in Figure 4N: DAPI labels the soma of the cord positioned above the neurites that project through the cord, and as reported elsewhere, there is no obvious cord lumen. We did not observe any 5HT+ cell bodies in the cord soma in the limited sections we examined. As observed in the whole mount (Figure 4M), there is a broad distribution of cell bodies projecting into the plexus, without any dorsoventral differences. The pharyngeal epithelium also shows a prominent plexus throughout the pharynx, yet only a few isolated cell bodies are associated with the endoderm in these sections. Sections in the anterior trunk show cell bodies sparsely scattered throughout the ectoderm with a thin ectodermal plexus that thickens ventrally, and the dorsal cord showing far fewer axons labelled than in the ventral cord. The endodermal plexus is very sparse (Figure 4O). In the posterior trunk, labelling of axons in the ventral cord is more prominent and a thin plexus is detected throughout the

epithelium with scattered, isolated cell bodies (Figure 4P,Q). No endodermal plexus was detected.

GABAergic neurons: We used a GABA polyclonal antibody to stain GABAergic neurons in juveniles, as has been previously demonstrated in another enteropneust species, *P. flava* (Nomaksteinsky et al., 2009). To address concerns about antibody binding specificity, we compared GABA antisera reactivity with the *in situ* hybridization for GAD (Figure 2). We observed good concordance between the antibody and *in situ* hybridization localizations. The GABAergic nervous system in juveniles is concentrated both in the anterior and posterior proboscis ectoderm (Figure 5A,Ai). In the collar, there are two ectodermal rings of cells at the lip of the collar (Figure 5A). In the trunk, there are isolated neurons along the dorsal midline in both the ectoderm and endoderm (Figure 5Aii). These cells appear similar in morphology to 5HT+ cells; bipolar with a single neurite extending from the cell body to the apical region terminating with an apical cilium, and the axon descending into the plexus on the basal side. There are also dorsal endodermal neurons with a neurite projecting to the apical surface of the endoderm, but with the cell body embedded in the endodermal plexus (Figure 5Aii). Further posteriorly, there are prominent axonal projections around the gill slits and into the ventral cord (Figure 5Aiii).

The number of cell bodies at the proboscis, collar, and trunk increases substantially in adults. The base of the proboscis forms a similar pattern of GABA+ neurite bundles to those detected from 1E11 and 5HT (Figure 5B). The adult collar has a more expansive concentration of neurons with the anterior ring and scattered cell bodies throughout the collar ectoderm (Figure 5C). GABAergic neurons are labeled in gill bars (Figure 5D) with cell bodies projecting axons ventrally. To directly image the dorsal cord, we dissected the cord from the ectodermal tissue, keeping the nerve bundles intact. This revealed many neurites projecting in an anterior-to-posterior direction along the length of the cord, with some neurites projecting laterally (Figure 5E).

FMRFamidergic nervous system**:** We used the rabbit polyclonal anti-FMRFamide to identify potential FMRFamidergic neurons in 3GS stage embryos. This antibody has been shown to be cross-reactive in a diverse set of bilaterians including echinoderms, where reactivity is observed in the radial nerve cord, tube feet, apical muscle, intestine, and the esophagus nerve plexus (Hoekstra et al., 2012). While the exact epitope that is recognized is uncertain, some studies have also found that the FMRFamide antibody exhibits cross-reactivity with SALMFamides and GFSKLYFamide in the sea cucumbers (Ajayi and Withyachumnarnkul, 2013; Diaz-Miranda et al., 1995). Therefore, the possible affinity to other neuropeptides must be considered in *S. kowalevskii.* The labelling shows significant overlap with the *in situ* data for PC2 and GPC, the two enzymes involved in the processing of neuropeptides, so this data provides information about the projection of a subset of neuropeptides within the complement in *S. kowalevskii*.

The peptidergic labelling from this antibody shows a broad circumferential distribution of neurons in the proboscis, but with a concentration at the proboscis base of both cell bodies and axons (Figure 5F). Neurons at the proboscis base have a flask-shaped morphology like the morphology of many other neurons described in this study, with a single cilium extending into the outer ectoderm (Figure 5F). These neurons appear to project posteriorly down the proboscis stem and along the dorsal collar cord, with some projections following the nerve plexus along the collar epithelium (Figure 5F, Fi) connecting with the ventral cord along the trunk (Figure 5F). Cell bodies are detected in the ventral cord with axons running the length of the cord. In the postanal tail of the juvenile, axons are clearly projecting anteriorly (Figure 5Fii). We examined

labelling of the adult nervous system by dissection of the ectoderm from the mesoderm in the proboscis and imaged the plexus (Figure 5G). This revealed an extensive plexus throughout the proboscis ectoderm with a general trend of bundled projections along the AP axis, but with many lateral neurites connecting these bundles projecting both long and short distances.

Neural transgenes:
In order to visualize neurons in higher resolution, we generated a Synapsin construct to drive expression of eGFP. Synapsin is a synaptic vesicle transmembrane protein and a marker of differentiated neurons (De Camilli et al., 1983; Huttner et al., 1983). Our construct was designed using 8 kilobases (KB) upstream of the start site of the synapsin-2-like gene (XP_006820290.1) (Minor et al., 2019). We examined transgene expression in over 50 F_0 juveniles at a range of developmental stages. The transgenic animals exhibit mosaic incorporation of the transgene and show neuronal staining most prominently throughout the proboscis ectoderm, sometimes in the dorsal region of the trunk and collar in isolated neurons (Figure 6A, B). Because of the mosaicism, transgenic animals ranged from a single labeled neuron to hundreds of labeled cells. From these transgenics animals, we identified the range of neural morphologies and the length and directionality of their neural processes. High magnification imaging of different regions along the AP axis reveals varicosities (Figure 6Ai) similar to the observations from DiI and antibody staining. The most common neural morphology we observed with this transgene were large bipolar sensory neurons, like those observed with 5HT immunohistochemistry. We found these neurons throughout the ectoderm, but at highest density in the proboscis. In a separate synapsin:GFP juveniles, we detect large bipolar neurons in the anterior tip of the proboscis projecting posteriorly towards the proboscis base (Figure 6B). At the dorsal proboscis base, neurons have a flask-shape morphology, with a rounded nucleus close to the neural plexus, and with either a single axon, white arrow in inset, or an axon that splits into an anteriorly and posteriorly projecting extension, grey arrow in inset (Figure 6Aii). We also identified a group of elongated sensory neurons in the posterior collar with a single axon projecting anteriorly into the cord, white arrows (Figure 6Aiii). Similar neural morphology was detected in the posterior ectoderm with clear anterior projections (Figure 6Aiv). The projections of this group of neurons are potentially involved in relaying posterior sensory information from the trunk to the anterior part of the animal with most axonal termini at the base of the proboscis. We rarely detected unipolar neurons, but one is shown associated with the plexus projecting anteriorly into the dorsal cord towards the proboscis, grey arrow (Figure 6Aiii). Elongated bipolar neurons are detected in the far posterior ectoderm and project anteriorly along the dorsal midline, likely along the dorsal cord (Figure 6Aiv).

Many of the bipolar neurons have prominent swellings along the axons projecting into the basiepithelial plexus (Figure 6Bi) similar to what we reported for DiI and serotonin. Many of these varicosities are located close to the basement membrane of the plexus, so it is possible that these boutons may be acting in a paracrine fashion, releasing transmitters/peptides locally modulating other neurons, directly stimulating muscles through the basement membrane, or representing *en passant* synapses within the plexus. In some cases, we detect what we interpret to be interneurons, closely associated with the neural plexus, co-labelled with DAPI (Figure 6Bii). We also find neurons with a more circular cell body morphology along the mid-proboscis that project anteriorly (Figure 6Biii). In this juvenile, bipolar neurons in the proboscis project posteriorly and appear to terminate at the proboscis base rather than extending further posteriorly (Figure 6B). In other transgenic juveniles, the population of bipolar neurons, right above the first gill slit in the anterior dorsal midline trunk, project anteriorly and terminate at the dorsal proboscis base in many of the animals that were imaged (Figure 6C).

Overall, based on the data from this synapsin transgene, the *S. kowalevskii* ectoderm contains a range of neural cell types including pseudounipolar, bipolar, multipolar, and multiciliated neurons in the proboscis and collar (Figure 6D-G). However, by far the most prevalent type of labeled neuron is the bipolar morphology observed throughout the animal. The abundant bipolar neurons are distinguishable from other types of cells in the ectoderm such as secretory, glial, and epithelial cells because of the distinctive axonal projections into the plexus.

Location of transmitter release: eGFP+ neurons from the transgene, DiI staining on fixed tissue, and NeuO labeling in live tissue, all reveal the presence of varicosities along the axons for most of the labelled neurons, most likely the site of transmitter/peptide release, possibly resulting in volumetric transmission or as *en passant* synapses. To further test this and to determine the localization of synapses/transmitter release throughout the nervous system, we designed a construct based on the previous synapsin:eGFP from Figure 6, but with the addition of a mouse synaptophysin-mRuby fusion protein. Synaptophysin is a presynaptic vesicle protein (Pennuto et al., 2003; Wiedenmann and Franke, 1985), so we expect the fusion protein to be transported to either synapses or regions of vesicle release, as has been demonstrated in mouse using a similar construct (Beier et al., 2015). The transgene generates mosaic eGFP expression similar to data presented in Figure 6 (Figure 7A,E). Within these eGFP-labelled neurons, we detect puncta labelled with mRuby, suggesting that the mouse Synaptophysin is trafficked successfully in hemichordates and labels regions of transmitter/peptide release. In the anterior proboscis (Figure 7B), there are many synaptophysin puncta along axons in addition to axon terminus containing a concentration of the synaptophysin fusion protein (Figure 2B,C,D). We observe broad distribution of these puncta in both the anterior (Figure 7B) and posterior proboscis (Figure 7C). Synaptophysin also shows localization around the nucleus and along the cilium in bipolar neurons (Figure 7D). In one striking example, we were able to track a single axon from a cell body in the far posterior to the mid proboscis (Figure 7E). Regular localization of Synaptophysin in swellings along the length of the axon supports our previous suggestion that the neuron is secreting transmitters/peptides locally or making direct neuron-to-neuron connections in the trunk plexus (Figure 7F-H).

Tyrosine hydroxylase

To investigate the cellular morphology and projections of catecholaminargic neurons, we designed a transgene using 5KB of sequence directly upstream of the tyrosine hydroxylase gene. Previously, we established that the cells expressing TH in the proboscis and collar also expressed the dopamine transporter (DAT) supporting the hypothesis that catecholaminergic TH-expressing cells are dopaminergic neurons (Figure 2). The TH:eGFP transgene expression is again expressed mosaically and mainly restricted to the proboscis, with a few isolated cells in the posterior collar (Figure 8A). Many of the labelled neurons in the proboscis have a flask-shaped morphology, as reported for synapsin:eGFP, and contain a single axonal projection directly into the plexus (Figure 8B,C,F,F'). In about half of the animals imaged, we identified a unique type of cell at the posterior collar and in many cases were able to trace their projections (Figure 8D,E). They have a unique asymmetric cellular morphology; a single dendrite with a terminal sensory cilium, and a protruding vacuole-rich mass. These cells have elaborate axonal trajectories across the collar and often project anteriorly into the proboscis (Figure 8G-I'). Individual neurons were traced and 3D-reconstructed using the 3D Visualization-Assisted Analysis (Vaa3D) software suite. TH transgene-labelled neurons in the anterior proboscis project posteriorly towards the proboscis base (Figure 8F,F') whereas eGFP+ neurons at the proboscis base project anteriorly towards the proboscis tip (Figure 8J-K'). Outside of the

proboscis in the few eGFP+ neurons in the collar, neurons project anteriorly towards the proboscis base (Figure 8G-I').

In summary, the transgenic data reveal the detailed cellular morphology of neurons across different regions of the body plan, and for the most part, neurons have a similar morphology; bipolar sensory neurons that project into the neural plexus and often at long distances. Far fewer neurons with detected with more diverse morphologies that were described in classical studies.

Discussion.

Distribution of neurons and neural cell types in *S. kowalevskii*.

The expression of a wide range of molecular markers of neurons and neural subtypes in *S. kowalevskii* confirms the broad distribution of neurons in the ectoderm outlined in several classical descriptions (Bullock, 1940; Bullock, 1945; Hess, 1937). Subsequent molecular studies have focused on the distribution of neurons in the cords, in particular the dorsal cord due the proposed affinities with the chordate dorsal cord. Our study provides additional insights, and the data clearly identifies the distribution of neurons of different types, but for a comprehensive picture of neural distribution, expression data from *elav*, a pan neural marker, needs to be integrated with more specific neural cell type markers, as some neurons in the epithelium are not *elav*+. The proboscis epithelium is the most richly innervated region of the animal, particularly at the base, and close to the proboscis stem on the dorsal side, as has been described in other species of enteropneust (Nomaksteinsky et al., 2009). The collar ectoderm is quite densely populated with neurons but the trunk far less so, but neurons are concentrated along the midlines in both the dorsal and ventral cords (Figure 1P,S).

The strongly regionalized distribution of neural subtype markers in the epithelium of both classical neurotransmitters and peptidergic neurons suggests that there is marked differentiation of the nervous system in both the AP and DV axes (Figure 2). At the late juvenile stages, we observed predominantly regionalized neural subtypes in the anterior plexus. However, we also saw evidence of clear molecular differentiation of neural subtypes between the dorsal and ventral cords, but in relatively few markers when compared with expression in the plexus. These data provide a broader view of neural cell type specification throughout the body plan rather than a focus on cord differentiation as in other studies (Miyamoto et al., 2010; Miyamoto and Wada, 2013; Nomaksteinsky et al., 2009).

General ectodermal regionalization: We observed the most complex regionalized patterns in the proboscis and collar epithelium, and far fewer in the trunk. In the proboscis, there were three general expression domains; apically restricted, broadly expressed, and localized to the base, with some markers represented in multiple domains. Most of these neural populations show circumferential domains with little evidence of dorsoventral differentiation reflective of the structure of the plexus. The base of the proboscis is both the region of highest neural density and the most diverse in terms of neural cell types. Dopamine (DA), GABA, histaminergic, and peptidergic neurons show strongly circumferentially localized domains of expression in this region (Figure 2), and as we highlight later, it is also one of the most distinctive regions of neural plexus organization (Figure 3). The expression of GABA in the proboscis of *P. flava* exhibited a similar distribution to our findings, although their focus was largely restricted to the base of the proboscis and stem (Nomaksteinsky et al., 2009). In the collar, the diversity and density of

neurons is less than in the proboscis, and in the trunk of late juveniles, the only 2 neural subtypes represented in the general ectoderm of late juveniles, not associated with the cords, are serotonin and DA.

The rings of neural subtypes in both the collar and proboscis ectoderm are very similar to the expression domains of the regulatory genes with conserved bilaterian roles in CNS patterning described in previous studies on *S. kowalevski* and other enteropneusts species (Kaul-Strehlow et al., 2017; Lowe et al., 2003; Pani et al., 2012). What is particularly striking is the clustering of neural subtypes in the regions of the ectoderm that are the sites of localized epithelial signaling centers during early development. The apical tip of the developing proboscis is the site of active FGF and hh signaling, and a source of Wnt antagonists (Darras et al., 2018; Pani et al., 2012). This territory and has been compared to the vertebrate anterior neural ridge. We observe a wide range of neural subtypes clustered in this region. At early developmental stages, the boundary between the proboscis and collar is the site of a narrow circumferential stripe of transitory hh expression that strongly resembles the regulatory gene expression profiles of the vertebrate Zona Limitans intrathalamica (ZLI). We notably observed a tight localization of GABA and DA neurons clustered in this region on either side of this organizer. Finally, the boundary of the collar and trunk is the site of the expression of Wnt1 and FGF8, which are the characteristic ligands of the isthmus organizer at the midbrain hindbrain organizer. This is a key organizer for the formation of the midbrain dopaminergic neurons in vertebrates, and both TH *in situs* and transgenics show TH neurons in this general region. Further functional tests will be required to determine whether these conserved regulatory networks are involved in the regulation of specific neural subtypes in these territories but raises the exciting possibility that conservation of gene regulatory networks between these disparate body plans is related to their role in the positioning of conserved cell types along the AP axis.

Cord regionalization: Both the dorsal and ventral cords show characteristic expression domains of specific neural cell types. However, we detect the expression of only a subset of the markers that we see prominently expressed in the proboscis. Despite fewer neural subtypes, those that are expressed show that the cords are distinct molecularly, suggesting differentiation of function. Given our analysis was largely restricted to late juveniles, it is possible that the complement of neural subtypes expands as the animals grow larger. The dorsal cord is divided into the internalized collar cord, and superficial cord than runs the length of the trunk to the anus. Surprisingly, we see little evidence of any neurotransmitter marker expression in the collar cord soma, except for peptidergic neurons, despite the prominent expression of *elav*. In the more posterior domains, where the cord is superficial and basiepidermal along the trunk, there are glutamatergic neurons that run down either side of the dorsal cord, and a few isolated GABA labelled cells in the anterior portion of the dorsal cord. Both cords, show clear expression of peptidergic neurons based on the expression of the processing enzymes and several neuropeptides. The length of the ventral cord shows strong and broad expression of the histidine marker HDC.

When the expression of a wide range of markers of neural differentiation are considered, in both the epidermis and in the cords, we see that most neurons at the late juvenile stage are in the proboscis ectoderm rather than in the cords. The region of the highest neural density and diversity is in the proboscis ectoderm, around the base. A previous study in *P. flava* (Nomaksteinsky et al., 2009) had identified the proboscis stem as a region with strong neural differentiation, and we also observed this, but we would include the entire proboscis base in this region of rich neural diversity rather than just the dorsal territory. Many of the gene expression

domains in this region are organized in circular rings reminiscent of the expression of nested transcription factors with key roles in neural cell fate determination in vertebrate brain development.

General organizational features of the plexus and cords

Previous studies have revealed the pervasive plexus present throughout the epidermis, and our data further refines the structural details of the plexus adding significant details (Bullock, 1945; Knight-Jones, 1952; Silèn, 1950; Spengel, 1877, 1903). The plexus is more prominent in the proboscis and with a striking change in organization at the proboscis base is the most striking, where its organization transitions from parallel nerve bundles running along the AP axis, into a mesh of axonal bundles containing both serotonergic, GABAergic, and peptidergic processes. A very similar plexus structure has recently been reported in different acoel species (Hulett et al., 2020). In these cases, it is reported that the reticulated neurite bundles wrap around cell clusters. Dilly (1969) reported that the enteropneust epithelium is strongly bound to the basement membrane by cellular processes that penetrate this plexus, so it is possible that this territory has its distinctive morphology due to cells penetrating and attaching to the basement membrane. The plexus is much thicker at the proboscis base and is most prominent on the dorsal side and possibly represents a center of integration (Nomaksteinsky et al., 2009). While this structure is most striking at the base of the proboscis, a looser mesh of axonal bundles is also present in the collar. Confocal z-stacks of the plexus, stained with neural antibodies or following DiI labelling, show that the plexus clearly has some apico/basal structural organization throughout the proboscis and collar suggestive of a partitioning of function – a scenario explicitly rejected in classical studies (Bullock, 1945).
Data from the transgenic embryos give particularly valuable insights into the structure of the plexus, as the mosaic incorporation of the transgene labels only a subset of neurons and enables the tracking of individual neurites/axons. We see no evidence of a plexus organization similar to that of the simple nets of cnidarians, in which local projections connect to neighboring neurons. Instead, we largely observe long range projections from sensory neurons in the epithelium. Neurons in the anterior proboscis mostly project posteriorly to the base of the proboscis. However, there is a wide range of axonal trajectories observed, and at the base of the proboscis we observed mostly lateral projections, but also some projections anteriorly. The few cells labelled in the trunk project anteriorly into the proboscis. In some experimental embryos, we were able to trace the neurite from the tip of the tail all the way up to the base of the proboscis, suggesting very long-range communication in the animal. We were unable to find a single instance of the axonal projections crossing the basement membrane and into the muscles, from either immunohistochemistry or transgenic data, representing a wide range of neural subtypes. This finding is significant as there has been some disagreement in the classical papers as to whether there is direct innervation of muscles and evidence of axonal processes crossing the basement membrane, summarized most recently by Dilly (1969). Light microscopy reports were decidedly mixed in their statements with some concluding they detected such processes but mostly were cautious and reserved in drawing conclusions (Bullock, 1945; Horst, 1939; Knight-Jones, 1952; Silèn, 1950). In Hyman's invertebrate treatise, she concluded there was no compelling evidence for fibers crossing the basement membrane (Hyman, 1955). With the advent of electron microscopy this issue was revisited: two independent studies suggest direct innervation of muscles from fibers crossing the basement membrane (Dilly, 1969; Nørrevang, 1965), but neither study report evidence of neuromuscular junctions. This question would clearly benefit from further clarification using modern serial approaches such as serial block face SEM (Lippens et al., 2019). Comprehensive examination

of the sister group to hemichordate, the echinoderms, has shown a similar lack of direct muscular innervation and penetration of the basement membrane by neural fibers in any echinoderm group examined (Cobb and Pentreath, 1977, 1978; Nieuwenhuys, 2000). Even in chordates, Amphioxus, the most basally branching chordate lineages, muscle fibers extend to the neural tube and stimulation occurs at this basement membrane interface (Flood, 1966), suggesting that sophisticated animal behavior can be mediated without a direct neuromuscular junction.

Our data further provides insights into the potential predominant mode of neural transmission in *S. kowalevskii*. The transgene and DiI data are particularly informative: all axons observed at high magnification were characterized by regular varicosities along their length. One striking Synapsin transgenic embryo showed regularly spaced varicosities along the axon of a single neuron from the tail all the way up into the base of the proboscis (Fig 7E-H)). Synaptophysin protein localized to the varicosities suggesting that transmitter/neuropeptide release occurs along the length of the neuron. Varicosities were also pervasive in the proboscis neurons lending support to the idea that, like in echinoderms, communication may largely be paracrine across the plexus, with general transmitter/neuropeptide volumetric release. Volumetric transmission is recognized as a critical component of a wide range of neural systems from the simple to the more complex (Descarries et al., 2008; Descarries et al., 1997; Descarries and Mechawar, 2000; Nicholson, 2000; Nieuwenhuys, 2000). In many extant nervous systems, from vertebrates to *C. elegans* and marine larvae, paracrine, chemically wired brain centers are integrated with synaptic networks, and some authors have proposed that most extant nervous systems likely evolved from peptidergic, paracrine systems (Jekely, 2021). We propose that during the early ambulacrarian evolution paracrine signaling was evolutionarily favored as the predominant mode of neural transmission. We cannot rule out the presence of true synapses between neurons in the plexus and the cords, but at least in the juveniles we examined the presence of neuromuscular junctions is unlikely, and we saw no evidence of the presence of axonal processes crossing the basement membrane into the muscle as was reported by early EM studies (Dilly, 1969). However, it is possible that these develop as the animals grow larger. Nieuwenhuys from his review of volumetric transmission across animal groups (Nieuwenhuys, 2000) makes the key statement that “the notion that volume transmission is primitive, generalized, sluggish and lacks precision, whereas wiring transmission is advanced, specialized, fast and accurate, is erroneous.” Our data needs to be corroborated by neurophysiological assays to determine the function of the nervous system in enteropneusts, but already sets up some clear hypotheses that can be further tested by some targeted serial EM to investigate the detailed structure in the plexus at a variety of regions of the body plan. Of course, this is a description of a single species representing one family of enteropneusts, and follow up studies in additional species representing a broader range of diversity will be required to determine whether the details of *S.kowalevskii* neuroanatomy adequately represents the main organizational features of enteropneusts.

Central or decentralized nervous system.

Much of the comparative interest in enteropneusts has been in its potential to provide insights into the early origins of chordates. The structure of the nervous system is a critical character for inferring ancestral states of early deuterostome nervous system (Holland et al., 2015). Our data provides some insights into this question, but also raises many others. A simple statement to satisfy whether enteropneusts are characterized by a central nervous system clearly delineated

from a peripheral nervous system seems largely driven by our expectations based on studies from highly derived, cephalized model animals. Our data does not provide a clear answer to the question.

The transgenic animals are the most informative on this issue as they reveal that the predominant neural cell type is a bipolar sensory neuron that project long distances, both in the proboscis and in the trunk. We found scant evidence of the multipolar neurons described in classical studies at the basal side of the plexus that may act as interneurons. In a few animals, we identified what we interpreted as a potential interneuron close to the predominant bipolar sensory neurons in the tip of the proboscis, and a few instances of multipolar neurons in the proboscis plexus (Figure 6). From our data so far, it is difficult to delineate a distinction between a clearly defined central nervous system and a peripheral nervous system. A previous molecular study (Nomaksteinsky et al., 2009) concluded that the dorsal cord and proboscis stem represented a “bonafide CNS” and the rest of the proboscis and remaining epithelium was a peripheral nervous system. Our data does not support such a strong division, as most neurons identified are sensory, with few candidates for interneurons. At least at this juvenile stage, a division between peripheral and central is not obvious, and the varicosities throughout the plexus are likely involved in processing sensory information. Our data does support an important role of the dorsal proboscis stem as a region of potential integration (Nomaksteinsky et al., 2009), as we observe many of axonal processes from transgenic embryos projecting to this region consistent with previous hypotheses, but the entire proboscis base may be a region of integration rather than simply the dorsal side. We find little support for a special role of the dorsal cord as an integrative center, but perhaps the cords take on more significant roles in processing as the animals grow as our data largely involved studies of late juveniles. However, the characterization of the rest of the proboscis representing a peripheral nervous separated from a central nervous system is not well supported. Our transgene data supports extensive release throughout the plexus, and may suggest that there is information processing throughout the plexus of the animal. The broad dispersal of many neurons, particularly in the proboscis and collar, also suggests that signal propagation occurs through tiling in a manner that has been proposed to represent ancestral nervous system function (Jékely 2021), and the characterization of the animal as having a “skin brain” may be the best analogy (Holland, 2003). Whether these varicosities represent true synapses or regions of volumetric release will require more detailed analysis with EM.

Experimental Procedures

Animal collection and embryo culture.

Adult worms were collected in the months of May and September during the *S. kowalevskii* breeding seasons in Waquoit Bay, MA., and maintained in flow-through sea tables at the Marine Biological Laboratory in Woods Hole, MA. Spawning fertilization and embryo culture followed protocols developed by Colwin and Colwin (1950, 1962) with updated methods (Lowe et al., 2004).

Cloning of orthologs

S. kowalevskii homologs of vertebrate genes were identified in an EST library screen (Freeman et al., 2008). See Supplemental Table 1 for NIH accession numbers.

In situ hybridization

Whole mount *in situ* hybridization on juveniles was carried out using an established lab protocol (Lowe et al., 2004). Embryos were kept in 5mL glass vials for all steps until the colorimetric reaction performed in 6 well tissue culture plates. Proteinase K treatment was carried out at 10µg/mL in PBTw for 15min at room temperature (RT). Acetic anhydride treatment at 250µM for 5min at RT followed by a 500µM treatment for 5 min at RT. *In situs* for experimental embryos were stained using 1.6µL:2.7µL ratio of 5-Bromo-4-chloro-3-indolyl phosphate**:** nitro-blue tetrazolium chloride and stopped with 3x5 minute rinses at RT in 1XMAB. Some samples were further cleared by rinsing 2×5 min in MeOH and cleared with a 2:1 ratio of benzyl benzoate: benzyl alcohol (BBBA) before imaging on a Zeiss Axioimager.

Whole mount *in situ* hybridizations on adults up to four gill slits utilized the same protocol as embryos with minor modifications: Samples were permeablized for 15-20 minutes at room temperature in Proteinase K diluted 1:7,500 in 1X PBST to increase probe penetration and staining in deeper tissues. The proboscis coelom and gut were punctured with a tungsten needle or scalpel blade to reduce probe trapping and increase penetration. For adult whole mount *in situ* hybridization, samples were dissected using a scalpel or scissors to reduce probe trapping and increase staining of deeper tissues. The whole mount *in situ* hybridization protocol was modified for adults by utilizing either large glass vials or 15 mL tubes and performing at least two more washes than embryos for all steps.

In situ hybridization on tissue sections was based on the protocol for embryos with technical modifications for slides. Fixed adults were dissected into pieces no more than 3 cm in length and cryoprotected in an increasing concentration gradient of sucrose in fixation buffer up to 20% sucrose at room temperature and allowed to equilibrate overnight at 4°C. Samples were then placed in 20% sucrose in fixation buffer diluted 2:1 in OCT media (Fisher) and allowed to equilibrate at room temperature with gentle agitation. Fixation buffer was utilized instead of 1X PBS to reduce tissue swelling and sectioning artifacts. Samples were embedded in plastic molds, chilled on dry ice, and stored indefinitely at -80°C. Frozen blocks were sectioned at 16-25 µm using a Leica cryostat with a cutting temperature between -25 and -30°C. Sections were collected on Superfrost Plus slides (Fisher), allowed to dry for at least 20 minutes, and either processed for *in situ* hybridizations or immunofluorescence immediately or stored at -80°C. Sections were permeablized with 0.2% Triton X-100 in 1X PBST for 20 minutes rather than with Proteinase K, and all washes were performed in upright slide mailers. For hybridization, sections were covered using plastic Hybrislip cover slips (Grace Technologies) and placed facing up in horizontal slide mailers with a Kimwipe or filter paper soaked in hybridization solution to prevent the slide from drying. Slide mailers were sealed using tape, placed in chambers constructed from empty pipette tip boxes, and hybridized overnight in an oven at 60°C. For blocking and antibody steps, sections were outlined using a hydrophobic marker, and incubations were performed on slides placed horizontally in humidified chambers at room temperature or at 4°C overnight. Different probes were hybridized in separate chambers.

Hybridization Chain Reaction (HCR) in situ hybridization: DNA probe sets were generated and ordered from Molecular Instruments, Inc. using the full RNA sequence from GeneBank accession numbers TH (XM_006813504.1), DAT (NM_001168055), VGLUT (XM_002739644), GAD (XM_002740628), achatin (XM_002732101.2), CCK (XM_002738068.2), and orexin (XM_002734948.2). 20 probe sets were generated for each gene, and DNA oligo pools were resuspended to a final concentration of 1µmol/µl in 50 mM Tris buffer, pH 7.5. HCR amplifiers, B1-Alexa Fluor-546, B2-Alexa Fluor-488, and B3-Alexa Fluor-647, were ordered from

Molecular Instruments, Inc. HCR version 3.0 protocol (Choi et al., 2018), and a protocol from Nipam Patels lab.

Immunohistochemistry

Juveniles were reared and fixed as previously described (Lowe et al., 2004) Briefly, embryos were fixed for 30 min at room temperature in fixation buffer (3.7% formaldehyde, 0.1 M MOPS pH 7.5, 0.5 M NaCl, 2 mM EGTA pH 8.0, 1 mM MgCl2, 1X PBS), and subsequently stored in ethanol at –20 °C. For anti-GABA, we used 3.7% formaldehyde and 0.3% glutaraldehyde. For antibody staining, embryos were rehydrated into 1x PBS +0.1% Triton X-100 (PBSTr), rinsed 3 × 10 min in PBSTr, and placed into a blocking solution of 1x PBS +0.1% Tween 20 (PBT) +5% goat serum for 2 h at room temperature. Embryos were incubated in PBT with either anti-GFP (Life Technologies, #A-6455), anti-FMRFamide (Immunostar, #20091), anti-5HT (Sigma, S5545), or anti-GABA (Sigma, A2052) at a 1:500 dilution overnight at 4 °C. After primary antibody incubation, embryos were washed 4 × 30 min in PBSTr, and then incubated for 4 h at room temperature with secondary antibody (Alexa-Fluor 488 goat anti-rabbit IgG, ThermoFisher #A-11008) diluted 1:500 in blocking solution. Samples were then washed 4 × 30 min in PBSTr and cleared into 80% glycerol. Some samples were further cleared by rinsing 2 × 5 min in MeOH and cleared with a 2:1 ratio of benzyl benzoate: benzyl alcohol (BBBA). Images were captured on a ZEIS LSM 700 confocal microscope with 20× and 40× objectives using the Zen software package (Carl Zeiss).

Immunofluorescence on adult tissue sections was performed as described previously with minor modifications. Sections were outlined with a hydrophobic marker, and wash steps were performed in an upright slide mailer. Blocking and antibody incubation steps were performed on slides placed horizontally in humidified chambers at room temperature. Primary antibody incubations were: 1E11, 1:3 (gift of Robert Burke); rabbit anti-serotonin, 1:250 (Sigma S5545); mouse anti-FMRFamide, 1:600 (Immunostar #20091). Secondary antibody (Molecular Probes) dilutions were: Alexa Fluor 488 goat anti-mouse or rabbit, 1:500; Alexa Fluor 546 goat anti-mouse or rabbit, 1:1000; Alexa Fluor goat anti-mouse or rabbit 647, 1:250. Imaging was performed using a Zeiss LSM700 confocal microscope with Zeiss Zen software, an Olympus FV1000 confocal microscope with Olympus software, or a Zeiss Axioimager.Z1 compound microscope or Discovery.V12 stereomicroscope with an Axiocam MRm camera and Zeiss Axiovision software.

Transgenes

5-8kb of putative promoters and enhancers sequence directly upstream of the start codon for genes TH (5kb, XM_006813504.1) and synapsin (8kb, XP_006820290.1) were cloned into a reporter plasmid based designed for developmental studies in Lampreys (Parker et al., 2014) containing I-SceI meganuclease restriction sites, upstream of an eGFP coding sequence and a SV40 late polyadenylation signal sequence using Gibson assembly (Gibson et al., 2009; Parker et al., 2014) and previously published (Minor et al., 2019). Full regulatory sequence for each transgene is included in Supplementary Table 1. Injection mixtures contained 10µl restriction digest including 5 units of I-SceI enzyme (NEB), 1µl CutSmart buffer, and 130ng of reporter plasmid, final concentration 13ng/µl. The mixture was incubated at 37 °C for 40 min and injected into embryos between 4-9 min post fertilization as previously described (Minor et al., 2019). To visualize regions of transmitter release, the mouse synaptophysin-mRuby fusion protein was cloned into the generated synapsin:eGFP transgene from AAV-FLExloxP-mGFP-2A-synaptophysin-mRuby (Addgene Plasmid# 71760) plasmid vector courtesy of Liqun Luo (Beier et al., 2015) to generate the synapsin:mGFP-2A-(mouse)synaptophysin-mRuby

transgene. Vector inset sequence and primers used for the generation of these plasmids are listed in Supplementary Table 1. Reconstruction of neural projections for a subset of neurons were generated using the 3D Visualization-Assisted Analysis (Vaa3D) software suite (Peng et al., 2014).

Acknowledgements.

We would like to thank the Staff of the Marine Biological Laboratory for hosting us and their assistance in pursuit of our research. The Waquoit National Estuarine Research Reserve for allowing access to our collection site. Jim Mcilvain from Zeiss for assistance in microscopy, Robb Krumlauf and Hugo Parker for providing the vector for our transgenics. Thurston Lacalli for his guidance and discussions on the evolutionary implications of this work, and Laurent Formery for his editorial input. This work was supported by a grant to an NSF grant (1656628) to CJL.

Figure Legends

Figure 1: Pan-neural marker, ELAV, expression.
(A) An illustration representing the transverse and sagittal sections taken along the adult body. (B, C) Transverse sections at the base of the proboscis show circumferential *elav* expression, with most extensive expression at the far proboscis base. (D-F) Anterior collar sections with dorsal to the right. (E) Higher magnification of the inset from D focused on the proboscis stem. *elav* staining in both the ectoderm and pharyngeal epithelium (PhEp) and in the anterior collar ring (ACR). (G-I) sections from the posterior collar with I showing a high magnification of inset from (H). (J) Section at the posterior trunk with expression in both dorsal (DNC) and ventral cords (VNC). (K-M) Sagittal sections from proboscis to anterior trunk. (K) Left of the midline, (L) on the midline showing the dorsal cord through the collar, and (M) to the right of the midline. (N, O) Late juvenile stage, whole mount. (N) Lateral view and (O), dorsal view of proboscis and collar. (P) *Elav* expression in dissected adult trunk ventral ectoderm showing the ventral cord. (Q) Whole mount adult proboscis dorsal view. (R) Dorsal view of adult anterior trunk. (S) Dorsal view of posterior trunk. Scale bars equal 250 μm, except in P-S 500 μm.

Figure 2: Expression of neural cell type markers
Gene expression in juvenile and adult tissue for components of neurotransmitter and neuropeptide signaling including synthesis and transport genes. (A-C) *Tyrosine Hydroxylase*. White arrowheads indicate expression at the base of the proboscis, open arrowhead at the tip of the collar, and black arrowhead at the anterior trunk. (A) Expression in early juvenile lateral view, (B) late juvenile lateral view. (C') Whole mount expression in adult proboscis, (C") lateral view of adult collar and base of proboscis. (D-E) coexpression of tyrosine hydroxylase and dopamine transporter in (D), early juvenile lateral view (AP – anterior proboscis, PB-proboscis base, and AC – anterior collar) with (D') a high magnification of the anterior proboscis, and (D"), a high magnification of the base of the proboscis. (E) Proboscis and collar of late juvenile. (F) Lateral view of an early juvenile showing expression of *tryptophan hydroxylase*. (G,H) Expression of *histidine decarboxylase* (white arrow indicates base of proboscis) in (G), early juvenile, and (H), late juvenile. (I-J) Expression of *vesicular glutamate transporter* in (I), early juvenile, lateral view with lower insight showing dorsal view of the collar and anterior trunk, (J'), dorsal view of later juvenile of the proboscis and collar and (J"), dorsal view of the trunk of a late juvenile. (K-M) Expression of *glutamate decarboxylase* in (K), early juvenile and (L), late juvenile in lateral view, (M'), whole mount of adult tip of the proboscis, (M"), dorsal view of the adult

collar and posterior proboscis. (N) Expression of *vesicular GABA transporter* in early juvenile. (O) *Proprotein convertase 2* expression in early juvenile lateral view, and (O'), expression in late juvenile, both in lateral view. (P) Expression of *glutaminyl-peptide cyclohydrolase* in P, early juvenile, and (P'), late juvenile. (Q) Expression of the neuropeptide NNFamide in (Q), early juvenile, and (Q'), late juvenile, both in lateral view. (R) Expression of neuropeptide WMRF-amide in (R), early juvenile, and (R'), late juvenile, both dorsal views. (S) Expression of Luqin in (S), early juvenile and (S'), late juvenile. (T) Expression of VLamide (VIG) in late juvenile showing the proboscis with a dorsal view, and with inset showing a lateral view. (U) *Achatin* expression in (U), early juvenile and (U') late juvenile, both lateral views, with only the proboscis and collar shown in (U'). (V) Cholecystokinin expression in late juvenile, lateral view. (W) *Orexin* expression in (W), early juvenile and (W') late juvenile, both lateral views. Scale bars are 100 μm in early juveniles, 200 μm in late juveniles, and 500 μm in adults.

Figure 3: Neural plexus organization
Visualization of the neural plexus in fixed and live tissue using an anti-synaptotagmin antibody (A-I), DiI (J-M), and Neo O (N). Juveniles are imaged in whole mount, and adult ectoderm by flat mount following dissection and imaging from the basal surface. (A) Maximum projection of a late juvenile stained for synaptotagmin (1E11), lateral view. (B) high magnification section of adult ectoderm at the base of the proboscis. (C) Illustration showing the performed excision of the posterior proboscis ectoderm from an adult animal. (D-I) Expression of synaptotagmin in dissected adult ectoderm in different regions of the body: (D) dorsal proboscis showing dorsal cord, (E) posterior proboscis base dissected as shown in (C), (F) anterior region of the proboscis base, (G) posterior region of the proboscis base, (H) the anterior collar, and (I) the dorsal trunk. (J-M) Lipophilic dye (DiI) injections into adult fixed tissue reveals dye diffusion across the adult plexus in (J) and (K), and neurite cell morphology in (L) and (M). (N) Live neural marker, NeuO, showing similar puncta along neurites seen in fixed tissue in (L) and (M). Scale bars represent 250 μm in A,D,E,I-K and 25 μm in B,F-H,L-N.

Figure 4: Serotonergic nervous system
Investigation of the serotinergic nervous system in juveniles (A-E) and adults (F-Q) using anti-5HT. (A) Maximum projection of a late juvenile lateral view. (B) High magnification of bipolar neurons with a sensory cilium projecting towards the apical region of the epithelium and a single neurite projecting basally into the neural plexus. (C-E) High magnification images from panels shown in (A): (C) posterior proboscis, (D) collar, and (E) trunk. Images are oriented in an anterior (left)-to-posterior(right) and a dorsal (up)-to-ventral(down) direction. (F-J) Adult ectoderm in the proboscis; (F) mid proboscis, (G, H) base of the proboscis double labelled with synaptotagmin, and the same specimen as in Fig 3E. (I) collar, and (J) trunk. (K) An illustration showing the sagittal sections carried out in adult tissues: All sections oriented with dorsal at the top of the panel with phalloidin labelled in purple, 5HT in white, and DAPI in blue. (L) proboscis, (M) mid-collar, (N) higher magnification of the dorsal collar cord, (O) anterior trunk, and (P) and (Q) showing the tail. Scale bars represent 500 μm in F,I,J,L,M, O-Q, 200 μm in A,G,N, 20 μm in B-E,H.

Figure 5: GABAergic and FMRFamidergic nervous system
Distribution of GABAergic and peptidergic neurons in juveniles and adults using anti-GABA and anti-FMRFamide polyclonal antibodies. (A-Aiii) distribution of GABA in juveniles. (A) Maximum projection of a late juvenile (Black arrows in A point to the ring of GABA neurons at the anterior collar), and higher magnification of the same individual at 3 different regions: (Ai) anterior proboscis, (Aii) anterior dorsal trunk (arrows indicating the dendrites projecting to the outer

epithelium of both the ectoderm and endoderm), and (Aiii) endodermal plexus in the pharyngeal gut of the anterior trunk, with neurites projecting around the gill slits (GS). (B-E) Dissected adult tissue at (B) the proboscis base, (C) collar, (D) gill slits at the trunk, and (E) dissected dorsal collar cord. (F) Maximum projection of a late juvenile labeled with anti-FMRF-amide, panels show the position of the subsequent high magnification images; Fi anterior collar and proboscis stem, (Fii) ventral trunk/ventral cord, and (Fiii) postanal tail. (G) Adult proboscis plexus. Scale bars are 100 μm, except 20 μm in panels Ai-Aiii, and Fi-Fiii.

Figure 6: Neural cell morphology and neurite projection
(A, B) Maximum projection of two representative synapsin:eGFP animals using 8kb regulatory sequence upstream of the synapsin I gene to drive expression of cytoplasmic eGFP. (Ai-Aiv) and (Bi-Bii) are high magnification panels for each juvenile revealing detailed cellular morphology and neurite projections. (Ai) The anterior proboscis plexus, red arrows point to varicosities along neurites. (Aii) The dorsal cord connecting the proboscis and collar, red arrow points to a single axon and green arrow points to a bifurcated axon from neurons projecting into the cord. (Aiii) Dorsal posterior collar, neurons projecting anteriorly along the dorsal collar cord, with red arrows indicating projecting axons. (Aiv) Postanal tail with detailed cellular morphology of neurons projecting anteriorly. (Bi) Anterior proboscis showing sensory cells projecting into the ectodermal plexus. (Bii) Pair of sensory cells in the apical tuft region that appear to project locally to interneuron in the plexus, indicated by red arrows. (Biii) Mid-proboscis with anteriorly projecting sensory neurons. (C) Projection trajectories from neurons in the dorsal posterior collar, right above the first gill slit, projecting anteriorly towards the dorsal proboscis base. (D-G) Representative neural cell type polarities across different animals. Scale bars in A,B represent 100 μm and 20 μm in Ai-G.

Figure 7: Localization of synaptophysin in varicosities
A, E Synapsin:mGFP—T2A—(mouse)Synaptophysin-mRuby expression from two representative animals using 8kb regulatory sequence upstream of the synapsin I gene to drive expression of mGFP and the mouse synaptophysin-mRuby fusion protein cleaved off by the self-cleaving enzyme sequence, T2A. Mosaic expression of Transgene in 2 representative animals Synaptophysin-mRuby (SYP-mRuby) expression is shown in green channel, synapsin:eGFP (SYN:eGFP) expression in magenta, and nuclear stain with DAPI in blue. (A) Transgene expression in the proboscis neural plexus with higher magnification in (B) anterior proboscis, (C) posterior proboscis base, and (D) dorsal posterior ectoderm. (E) Second animal showing a single neuron expressing the transgene, dorsal view. The cell body is in the tail and projects into the proboscis. (F-H) Higher magnification panels along the length neuron: (F) neural cell body, (G) mid-axon at the dorsal posterior collar, (H) axon terminal at the mid-proboscis. G', H', and H'' are higher magnification images to show SYP-mRuby puncta along the axon, H' is the axon terminal. Scale bars in A,E are 100 μm and 20μm in B-D, and F-H'.

Figure 8: TH:GFP transgene
(A) Maximum projection of a TH:eGFP representative animal using 5KB regulatory sequence upstream of the TH gene to drive expression of cytoplasmic eGFP. (B-D) Higher magnification images at (B) anterior proboscis, (C) ventral posterior proboscis, and (D) ventral collar. (E) Proboscis ectoderm from a different animal showing detailed cellular morphology of TH+ neurons. (F-K') Manually traced axons from sensory neurons that project posteriorly in the proboscis (F, F'), collar neurons that project anteriorly towards the proboscis (G-I'), and proboscis base neurons that project anteriorly towards the proboscis tip (J-K'). Scale bars in A represent 100 μm, 50 μm in F-K, and 20 μm in B-E and F'-K'.

Supplemental Table:
NIH accession numbers for *S. kowalevskii* homologs of vertebrate genes identified in an EST library screen (Freeman et al., 2008).

Supplemental Movie 1:
A Z-stack along the trunk of an adult clearly showing the layered nature of the plexus against the synaptotagmin 1 (1E11) antibody.

Supplemental Movie 2:
A Z-stack along the collar and trunk of a 3GS juvenile. The 5HT antibody clearly showing the serotonergic nervous system composed of many sensory neurons at the collar and trunk with a basipethelial neuro plexus.

References

Ajayi, A., Withyachumnarnkul, B., 2013. Presence and distribution of FMRFamide-like immunoreactivity in the sea cucumber Holothuria scabra (Jaeger, 1833). Zoomorphology 132, 285-300.
Antzoulatos, E.G., Byrne, J.H., 2004. Learning insights transmitted by glutamate. Trends Neurosci 27, 555-560.
Arendt, D., Nubler-Jung, K., 1994. Inversion of dorsoventral axis? Nature 371, 26.
Arendt, D., Nubler-Jung, K., 1996. Common ground plans in early brain development in mice and flies. Bioessays 18, 255-259.
Aronowicz, J., Lowe, C.J., 2006. Hox gene expression in the hemichordate Saccoglossus kowalevskii and the evolution of deuterostome nervous systems. Integrative and comparative biology 46, 890-901.
Bateson, W., 1885. Later stages in the development of Balanoglossus Kowalevskii with a suggestion as to the affinities of the Enteropneusta. Quarterly Journal of Microscopical Science 25, 81-128.
Bateson, W., 1886. The ancestry of the chordata. Quarterly Journal of Microscopical Science 26, 535-571.
Beier, K.T., Steinberg, E.E., DeLoach, K.E., Xie, S., Miyamichi, K., Schwarz, L., Gao, X.J., Kremer, E.J., Malenka, R.C., Luo, L., 2015. Circuit Architecture of VTA Dopamine Neurons Revealed by Systematic Input-Output Mapping. Cell 162, 622-634.
Bromham, L.D., Degnan, B.M., 1999. Hemichordates and deuterostome evolution: robust molecular phylogenetic support for a hemichordate + echinoderm clade. Evolution & development 1, 166-171.
Brown, F.D., Prendergast, A., Swalla, B.J., 2008. Man is but a worm: chordate origins. Genesis 46, 605-613.
Bullock, T.H., 1940. The functional organisation of the nervous system of the Enteropneusta. Biological Bulletin 79, 91.
Bullock, T.H., 1944. The giant nerve fibre system in Balanoglossids. J. Comp. Neurol. 80, 355.
Bullock, T.H., 1945. The anatomical organization of the nervous system of enteropneusta. Quart. J. Microscrop. Sci. 86, 55-112.

Bullock, T.H., Horridge, G.A., 1965. Structure and function in the nervous systems of invertebrates. W. H. Freeman, San Francisco,.
Burbach, J.P., 2011. What are neuropeptides? Methods Mol Biol 789, 1-36.
Busby, W.H., Jr., Quackenbush, G.E., Humm, J., Youngblood, W.W., Kizer, J.S., 1987. An enzyme(s) that converts glutaminyl-peptides into pyroglutamyl-peptides. Presence in pituitary, brain, adrenal medulla, and lymphocytes. J Biol Chem 262, 8532-8536.
Byrne, M., Nakajima, Y., Chee, F.C., Burke, R.D., 2007. Apical organs in echinoderm larvae: insights into larval evolution in the Ambulacraria. Evolution & development 9, 432-445.
Cameron, C.B., Garey, J.R., Swalla, B.J., 2000. Evolution of the chordate body plan: new insights from phylogenetic analyses of deuterostome phyla. Proc Natl Acad Sci U S A 97, 4469-4474.
Cannon, J.T., Kocot, K.M., Waits, D.S., Weese, D.A., Swalla, B.J., Santos, S.R., Halanych, K.M., 2014. Phylogenomic resolution of the hemichordate and echinoderm clade. Curr Biol 24, 2827-2832.
Choi, H.M.T., Schwarzkopf, M., Fornace, M.E., Acharya, A., Artavanis, G., Stegmaier, J., Cunha, A., Pierce, N.A., 2018. Third-generation in situ hybridization chain reaction: multiplexed, quantitative, sensitive, versatile, robust. Development 145.
Cobb, J.L., Pentreath, V.W., 1977. Anatomical studies of simple invertebrate synapses utilizing stage rotation election microscopy and densitometry. Tissue Cell 9, 125-135.
Cobb, J.L., Pentreath, V.W., 1978. Comparison of the morphology of synapses in invertebrate and vertebrate nervous systems: analysis of the significance of the anatomical differences and interpretation of the morphological specializations. Prog Neurobiol 10, 231-252.
Cunningham, D., Casey, E.S., 2014. Spatiotemporal development of the embryonic nervous system of Saccoglossus kowalevskii. Dev Biol 386, 252-263.
Danbolt, N.C., 2001. Glutamate uptake. Prog Neurobiol 65, 1-105.
Darras, S., Fritzenwanker, J.H., Uhlinger, K.R., Farrelly, E., Pani, A.M., Hurley, I.A., Norris, R.P., Osovitz, M., Terasaki, M., Wu, M., Aronowicz, J., Kirschner, M., Gerhart, J.C., Lowe, C.J., 2018. Anteroposterior axis patterning by early canonical Wnt signaling during hemichordate development. PLoS Biol 16, e2003698.
Dawydoff, C., 1948. Classe des Entéropneustes., in: Grassé, P.P. (Ed.), Traité de Zoologie, Paris: Libraries de l'Academie de Médecine, pp. 369-453
.
De Camilli, P., Harris, S.M., Jr., Huttner, W.B., Greengard, P., 1983. Synapsin I (Protein I), a nerve terminal-specific phosphoprotein. II. Its specific association with synaptic vesicles demonstrated by immunocytochemistry in agarose-embedded synaptosomes. J Cell Biol 96, 1355-1373.
de Castro, F., 1950. Die Normale Histologie des Peripheren Vegetativen Nervensystems: Das Synapsen-Problem Anatomisch-experimentelle UntersuchungAnatomisch-experimentelle Untersuchung. Julius Springer.
De Robertis, E.M., 2008. Evo-devo: variations on ancestral themes. Cell 132, 185-195.
De Robertis, E.M., Sasai, Y., 1996. A common plan for dorsoventral patterning in Bilateria. Nature 380, 37-40.
Denes, A.S., Jekely, G., Steinmetz, P.R., Raible, F., Snyman, H., Prud'homme, B., Ferrier, D.E., Balavoine, G., Arendt, D., 2007. Molecular architecture of annelid nerve cord supports common origin of nervous system centralization in bilateria. Cell 129, 277-288.

Descarries, L., Berube-Carriere, N., Riad, M., Bo, G.D., Mendez, J.A., Trudeau, L.E., 2008. Glutamate in dopamine neurons: synaptic versus diffuse transmission. Brain Res Rev 58, 290-302.
Descarries, L., Gisiger, V., Steriade, M., 1997. Diffuse transmission by acetylcholine in the CNS. Prog Neurobiol 53, 603-625.
Descarries, L., Mechawar, N., 2000. Ultrastructural evidence for diffuse transmission by monoamine and acetylcholine neurons of the central nervous system. Prog Brain Res 125, 27-47.
Diaz-Miranda, L., Blanco, R.E., Garcia-Arraras, J.E., 1995. Localization of the heptapeptide GFSKLYFamide in the sea cucumber Holothuria glaberrima (Echinodermata): a light and electron microscopic study. J Comp Neurol 352, 626-640.
Dilly, P.N., 1969. The nerve fibres in the basement membrane and related structures in Saccoglossus horsti (Enteropneusta). Z Zellforsch Mikrosk Anat 97, 69-83.
Dilly, P.N., Welsch, U., Storch, V., 1970. The structure of the nerve fiber layer and neurocord in the enteropneusts. . Z. Zellforsch. Mikrosk. Anat. 103, 129-148.
Elphick, M.R., 2010. NG peptides: a novel family of neurophysin-associated neuropeptides. Gene 458, 20-26.
Elphick, M.R., Mirabeau, O., 2014. The Evolution and Variety of RFamide-Type Neuropeptides: Insights from Deuterostomian Invertebrates. Front Endocrinol (Lausanne) 5, 93.
Elphick, M.R., Mirabeau, O., Larhammar, D., 2018. Evolution of neuropeptide signalling systems. J Exp Biol 221.
Er, J.C., Leong, C., Teoh, C.L., Yuan, Q., Merchant, P., Dunn, M., Sulzer, D., Sames, D., Bhinge, A., Kim, D., Kim, S.M., Yoon, M.H., Stanton, L.W., Je, S.H., Yun, S.W., Chang, Y.T., 2015. NeuO: a fluorescent chemical probe for live neuron labeling. Angew Chem Int Ed Engl 54, 2442-2446.
Fischer, W.H., Spiess, J., 1987. Identification of a mammalian glutaminyl cyclase converting glutaminyl into pyroglutamyl peptides. Proc Natl Acad Sci U S A 84, 3628-3632.
Flood, P.R., 1966. A peculiar mode of muscular innervation in Amphioxus. Light and electron microscopic studies of the so-called ventral roots. J Comp Neurol 126, 181-217.
Fonnum, F., 1984. Glutamate: a neurotransmitter in mammalian brain. J Neurochem 42, 1-11.
Furlong, R.F., Holland, P.W., 2002. Bayesian phylogenetic analysis supports monophyly of ambulacraria and of cyclostomes. Zoolog Sci 19, 593-599.
Garstang, W., 1894. Preliminary note on a new theory of the phylogeny of the chordata. Zool. Anzeiger 22, 122-125.
Garstang, W., 1928. The morphology of the Tunicata. Quart J. Miscroscop. Sci. 72, 51-189.
Geoffroy-St. Hilaire, E., 1822. Considérations générales sur les vertebrés. Mem. HIst. Nat. 9, 89-119.
Gerschenfeld, H.M., 1973. Chemical transmission in invertebrate central nervous systems and neuromuscular junctions. Physiol Rev 53, 1-119.
Gibson, D.G., Young, L., Chuang, R.Y., Venter, J.C., Hutchison, C.A., 3rd, Smith, H.O., 2009. Enzymatic assembly of DNA molecules up to several hundred kilobases. Nat Methods 6, 343-345.
Gonzalez, P., Uhlinger, K.R., Lowe, C.J., 2017. The Adult Body Plan of Indirect Developing Hemichordates Develops by Adding a Hox-Patterned Trunk to an Anterior Larval Territory. Curr Biol 27, 87-95.

Greer, J.B., Khuri, S., Fieber, L.A., 2017. Phylogenetic analysis of ionotropic L-glutamate receptor genes in the Bilateria, with special notes on Aplysia californica. BMC Evol Biol 17, 11.
Hejnol, A., Lowe, C.J., 2015. Embracing the comparative approach: how robust phylogenies and broader developmental sampling impacts the understanding of nervous system evolution. Philos Trans R Soc Lond B Biol Sci 370.
Hess, W.N., 1937. The nervous system of Dolichoglossus kowalevskyi. Journal of Experimental Zoology 79, 1-11.
Hewes, R.S., Taghert, P.H., 2001. Neuropeptides and neuropeptide receptors in the Drosophila melanogaster genome. Genome Res 11, 1126-1142.
Hirth, F., 2010. On the origin and evolution of the tripartite brain. Brain Behav Evol 76, 3-10.
Hirth, F., Reichert, H., 1999. Conserved genetic programs in insect and mammalian brain development. Bioessays 21, 677-684.
Hoekstra, L.A., Moroz, L.L., Heyland, A., 2012. Novel insights into the echinoderm nervous system from histaminergic and FMRFaminergic-like cells in the sea cucumber Leptosynapta clarki. PLoS One 7, e44220.
Holland, L.Z., 2015. Evolution of basal deuterostome nervous systems. J Exp Biol 218, 637-645.
Holland, N.D., 2003. Early central nervous system evolution: an era of skin brains? Nat Rev Neurosci 4, 617-627.
Holland, N.D., Holland, L.Z., Holland, P.W., 2015. Scenarios for the making of vertebrates. Nature 520, 450-455.
Horst, C.J.v.d., 1939. Hemichordata. Akademische Verlagsgesellschaft m.b.H., Leipzig.
Hulett, R.E., Potter, D., Srivastava, M., 2020. Neural architecture and regeneration in the acoel Hofstenia miamia. Proceedings. Biological sciences / The Royal Society 287, 20201198.
Huttner, W.B., Schiebler, W., Greengard, P., De Camilli, P., 1983. Synapsin I (protein I), a nerve terminal-specific phosphoprotein. III. Its association with synaptic vesicles studied in a highly purified synaptic vesicle preparation. J Cell Biol 96, 1374-1388.
Hyman, L.H., 1955. The invertebrates, 1st ed. McGraw-Hill, New York,.
Jackson, F.R., Newby, L.M., Kulkarni, S.J., 1990. Drosophila GABAergic systems: sequence and expression of glutamic acid decarboxylase. J Neurochem 54, 1068-1078.
Jekely, G., 2013. Global view of the evolution and diversity of metazoan neuropeptide signaling. Proc Natl Acad Sci U S A 110, 8702-8707.
Jekely, G., 2021. The chemical brain hypothesis for the origin of nervous systems. Philos Trans R Soc Lond B Biol Sci 376, 20190761.
Kaul, S., Stach, T., 2010. Ontogeny of the collar cord: neurulation in the hemichordate Saccoglossus kowalevskii. J Morphol 271, 1240-1259.
Kaul-Strehlow, S., Röttinger, E., 2015. Hemichordata, in: Wanninger, A. (Ed.), Evolutionary Developmental Biology of Invertebrates 6: Deuterostomia. Springer Vienna, Vienna, pp. 59-89.
Kaul-Strehlow, S., Stach, T., 2013. A detailed description of the development of the hemichordate Saccoglossus kowalevskii using SEM, TEM, Histology and 3D-reconstructions. Frontiers in Zoology 10, 1-31.
Kaul-Strehlow, S., Urata, M., Minokawa, T., Stach, T., Wanninger, A., 2015. Neurogenesis in directly and indirectly developing enteropneusts: of nets and cords. Org Divers Evol 15, 405-422.

Kaul-Strehlow, S., Urata, M., Praher, D., Wanninger, A., 2017. Neuronal patterning of the tubular collar cord is highly conserved among enteropneusts but dissimilar to the chordate neural tube. Sci Rep 7, 7003.
Kinjo, A., Koito, T., Kawaguchi, S., Inoue, K., 2013. Evolutionary history of the GABA transporter (GAT) group revealed by marine invertebrate GAT-1. PLoS One 8, e82410.
Knight-Jones, E., 1952. On the nervous system of Saccoglossus cambriensis (Enteropneusta). . Philos. Trans. R. Soc. Lond. B. Biol. Sci. 236, 315-354.
Kowalevsky, A., 1866. Anatomie des Balanoglossus. Mem Acad Imp Sci St Petersburg 7, 16.
Krishnan, A., Almen, M.S., Fredriksson, R., Schioth, H.B., 2013. Remarkable similarities between the hemichordate (Saccoglossus kowalevskii) and vertebrate GPCR repertoire. Gene 526, 122-133.
Lichtneckert, R., Reichert, H., 2005. Insights into the urbilaterian brain: conserved genetic patterning mechanisms in insect and vertebrate brain development. Heredity (Edinb) 94, 465-477.
Lippens, S., Kremer, A., Borghgraef, P., Guerin, C.J., 2019. Serial block face-scanning electron microscopy for volume electron microscopy. Methods Cell Biol 152, 69-85.
Lowe, C.J., 2021. Molecular insights into deuterostome evolution from hemichordate developmental biology. Curr Top Dev Biol 141, 75-117.
Lowe, C.J., Tagawa, K., Humphreys, T., Kirschner, M., Gerhart, J., 2004. Hemichordate embryos: procurement, culture, and basic methods. Methods Cell Biol 74, 171-194.
Lowe, C.J., Terasaki, M., Wu, M., Freeman, R.M., Jr., Runft, L., Kwan, K., Haigo, S., Aronowicz, J., Lander, E., Gruber, C., Smith, M., Kirschner, M., Gerhart, J., 2006. Dorsoventral patterning in hemichordates: insights into early chordate evolution. PLoS Biol 4, e291.
Lowe, C.J., Wu, M., Salic, A., Evans, L., Lander, E., Stange-Thomann, N., Gruber, C.E., Gerhart, J., Kirschner, M., 2003. Anteroposterior patterning in hemichordates and the origins of the chordate nervous system. Cell 113, 853-865.
Luo, L., 2020. Principles of neurobiology, Second edition. ed. Garland Science, Boca Raton.
Luttrell, S., Konikoff, C., Byrne, A., Bengtsson, B., Swalla, B.J., 2012. Ptychoderid hemichordate neurulation without a notochord. Integrative and comparative biology 52, 829-834.
Martin-Duran, J.M., Pang, K., Borve, A., Le, H.S., Furu, A., Cannon, J.T., Jondelius, U., Hejnol, A., 2018. Convergent evolution of bilaterian nerve cords. Nature 553, 45-50.
McIntire, S.L., Jorgensen, E., Kaplan, J., Horvitz, H.R., 1993. The GABAergic nervous system of Caenorhabditis elegans. Nature 364, 337-341.
Metschnikoff, V.E., 1881. Über die systematische Stellung von Balanoglossus. Zool Anz 4, 139-157.
Miller, M.W., 2019. GABA as a Neurotransmitter in Gastropod Molluscs. Biol Bull 236, 144-156.
Minor, P.J., Clarke, D.N., Andrade Lopez, J.M., Fritzenwanker, J.H., Gray, J., Lowe, C.J., 2019. I-SceI Meganuclease-mediated transgenesis in the acorn worm, Saccoglossus kowalevskii. Dev Biol 445, 8-15.
Mirabeau, O., Joly, J.S., 2013. Molecular evolution of peptidergic signaling systems in bilaterians. Proc Natl Acad Sci U S A 110, E2028-2037.
Miyamoto, N., Nakajima, Y., Wada, H., Saito, Y., 2010. Development of the nervous system in the acorn worm Balanoglossus simodensis: insights into nervous system evolution. Evolution & development 12, 416-424.

Miyamoto, N., Wada, H., 2013. Hemichordate neurulation and the origin of the neural tube. Nature communications 4, 2713.
Morgan, T., 1894. Development of Balanoglossus. Journal of Morphology 9, 1-86.
Mueller, T., Vernier, P., Wullimann, M.F., 2006. A phylotypic stage in vertebrate brain development: GABA cell patterns in zebrafish compared with mouse. J Comp Neurol 494, 620-634.
Nakajima, Y., Humphreys, T., Kaneko, H., Tagawa, K., 2004a. Development and neural organization of the tornaria larva of the Hawaiian hemichordate, Ptychodera flava. Zoolog Sci 21, 69-78.
Nakajima, Y., Kaneko, H., Murray, G., Burke, R.D., 2004b. Divergent patterns of neural development in larval echinoids and asteroids. Evolution & development 6, 95-104.
Nicholson, C., 2000. Volume transmission in the year 2000. Prog Brain Res 125, 437-446.
Nieuwenhuys, R., 2000. Comparative aspects of volume transmission, with sidelight on other forms of intercellular communication. Prog Brain Res 125, 49-126.
Nistri, A., Constanti, A., 1979. Pharmacological characterization of different types of GABA and glutamate receptors in vertebrates and invertebrates. Prog Neurobiol 13, 117-235.
Nomaksteinsky, M., Rottinger, E., Dufour, H.D., Chettouh, Z., Lowe, C.J., Martindale, M.Q., Brunet, J.F., 2009. Centralization of the deuterostome nervous system predates chordates. Curr Biol 19, 1264-1269.
Nørrevang, A., 1965. Fine structure of nervous layer, basement membrane, and muscles of the proboscis in Harrimania kupfferi (Enteropneusta). Vidensk. Medd. fra Dansk naturh. Foren. 128, 325-337.
Pani, A.M., Mullarkey, E.E., Aronowicz, J., Assimacopoulos, S., Grove, E.A., Lowe, C.J., 2012. Ancient deuterostome origins of vertebrate brain signalling centres. Nature 483, 289-294.
Parker, H.J., Bronner, M.E., Krumlauf, R., 2014. A Hox regulatory network of hindbrain segmentation is conserved to the base of vertebrates. Nature 514, 490-493.
Peng, Hanchuan, Alessandro Bria, Zhi Zhou, Giulio Iannello, and Fuhui Long. "Extensible visualization and analysis for multidimensional images using Vaa3D." *Nature protocols* 9, no. 1 (2014): 193-208.
Pennuto, M., Bonanomi, D., Benfenati, F., Valtorta, F., 2003. Synaptophysin I controls the targeting of VAMP2/synaptobrevin II to synaptic vesicles. Mol Biol Cell 14, 4909-4919.
Pham, K., Hobert, O., 2019. Unlike Drosophila elav, the C. elegans elav orthologue exc-7 is not panneuronally expressed. MicroPubl Biol 2019.
Roberts, E., Chase, T.N., Tower, D.B., City of Hope National Medical Center (U.S.), National Institute of Neurological and Communicative Disorders and Stroke., Kroc Foundation., 1976. GABA in nervous system function. Raven Press, New York.
Roberts, E., Kuriyama, K., 1968. Biochemical-physiological correlations in studies of the gamma-aminobutyric acid system. Brain Res 8, 1-35.
Robinow, S., Campos, A.R., Yao, K.M., White, K., 1988. The elav gene product of Drosophila, required in neurons, has three RNP consensus motifs. Science 242, 1570-1572.
Robinow, S., White, K., 1988. The locus elav of Drosophila melanogaster is expressed in neurons at all developmental stages. Dev Biol 126, 294-303.

Rouille, Y., Duguay, S.J., Lund, K., Furuta, M., Gong, Q., Lipkind, G., Oliva, A.A., Jr., Chan, S.J., Steiner, D.F., 1995. Proteolytic processing mechanisms in the biosynthesis of neuroendocrine peptides: the subtilisin-like proprotein convertases. Front Neuroendocrinol 16, 322-361.
Sanfilippo, P., Smibert, P., Duan, H., Lai, E.C., 2016. Neural specificity of the RNA-binding protein Elav is achieved by post-transcriptional repression in non-neural tissues. Development 143, 4474-4485.
Sato, A., Bishop, J.D., Holland, P.W., 2008. Developmental biology of pterobranch hemichordates: history and perspectives. Genesis 46, 587-591.
Seidah, N.G., Benjannet, S., Hamelin, J., Mamarbachi, A.M., Basak, A., Marcinkiewicz, J., Mbikay, M., Chretien, M., Marcinkiewicz, M., 1999. The subtilisin/kexin family of precursor convertases. Emphasis on PC1, PC2/7B2, POMC and the novel enzyme SKI-1. Ann N Y Acad Sci 885, 57-74.
Silèn, L., 1950. On the nervous system of Glossibalanus marginatus Meek (Enteropneusta). . Acta Zoologica 31, 149-175.
Spengel, J.W., 1877. Ueber den Bau und die Entwickelung des Balanoglossus. Amtl. Ber. 50,vers.d. Naturf. U. Artz, 176-177.
Spengel, J.W., 1903. Neue Betrage zur Kenntniss der Enteropneusta. !. Ptychodera flava. Zool. Jahrb., Abt. f. Anat. 18, 271-326.
Tassia, M.G., Cannon, J.T., Konikoff, C.E., Shenkar, N., Halanych, K.M., Swalla, B.J., 2016. The Global Diversity of Hemichordata. PLoS One 11, e0162564.
Tessmar-Raible, K., Raible, F., Christodoulou, F., Guy, K., Rembold, M., Hausen, H., Arendt, D., 2007. Conserved sensory-neurosecretory cell types in annelid and fish forebrain: insights into hypothalamus evolution. Cell 129, 1389-1400.
Tinoco, A.B., Barreiro-Iglesias, A., Yanez Guerra, L.A., Delroisse, J., Zhang, Y., Gunner, E.F., Zampronio, C.G., Jones, A.M., Egertova, M., Elphick, M.R., 2021. Ancient role of sulfakinin/cholecystokinin-type signalling in inhibitory regulation of feeding processes revealed in an echinoderm. Elife 10.
van den Pol, A.N., 2012. Neuropeptide transmission in brain circuits. Neuron 76, 98-115.
Walker, R.J., Papaioannou, S., Holden-Dye, L., 2009. A review of FMRFamide- and RFamide-like peptides in metazoa. Invert Neurosci 9, 111-153.
Watanabe, T., Taguchi, Y., Shiosaka, S., Tanaka, J., Kubota, H., Terano, Y., Tohyama, M., Wada, H., 1984. Distribution of the histaminergic neuron system in the central nervous system of rats; a fluorescent immunohistochemical analysis with histidine decarboxylase as a marker. Brain Res 295, 13-25.
Wiedenmann, B., Franke, W.W., 1985. Identification and localization of synaptophysin, an integral membrane glycoprotein of Mr 38,000 characteristic of presynaptic vesicles. Cell 41, 1017-1028.
Yao, Y., Minor, P.J., Zhao, Y.T., Jeong, Y., Pani, A.M., King, A.N., Symmons, O., Gan, L., Cardoso, W.V., Spitz, F., Lowe, C.J., Epstein, D.J., 2016. Cis-regulatory architecture of a brain signaling center predates the origin of chordates. Nat Genet 48, 575-580.
Zhang, X., Pan, H., Peng, B., Steiner, D.F., Pintar, J.E., Fricker, L.D., 2010. Neuropeptidomic analysis establishes a major role for prohormone convertase-2 in neuropeptide biosynthesis. J Neurochem 112, 1168-1179.

Figure 1

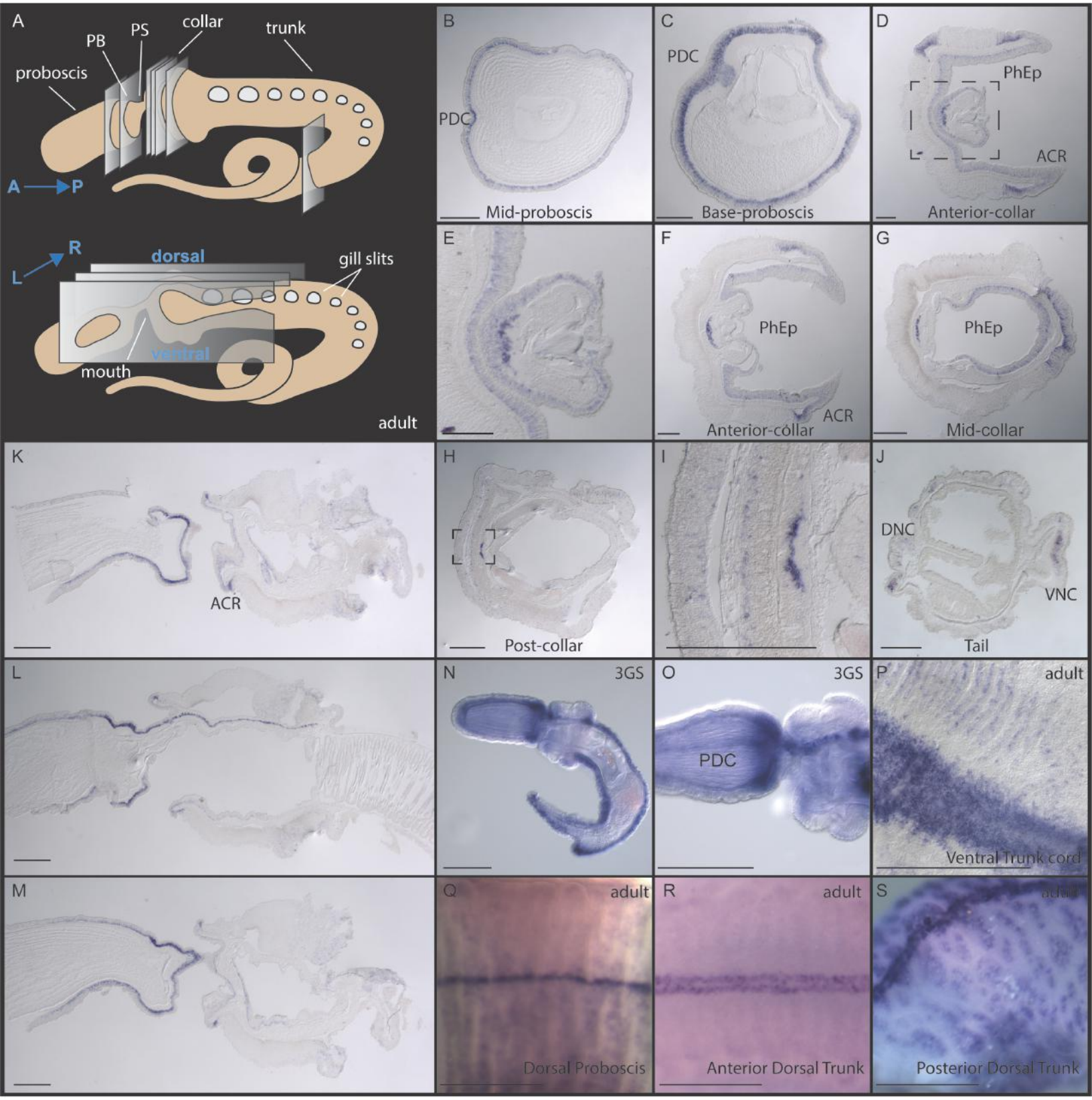

Adult scale bar: 500um
3GS scale bar: 250um

Figure 2

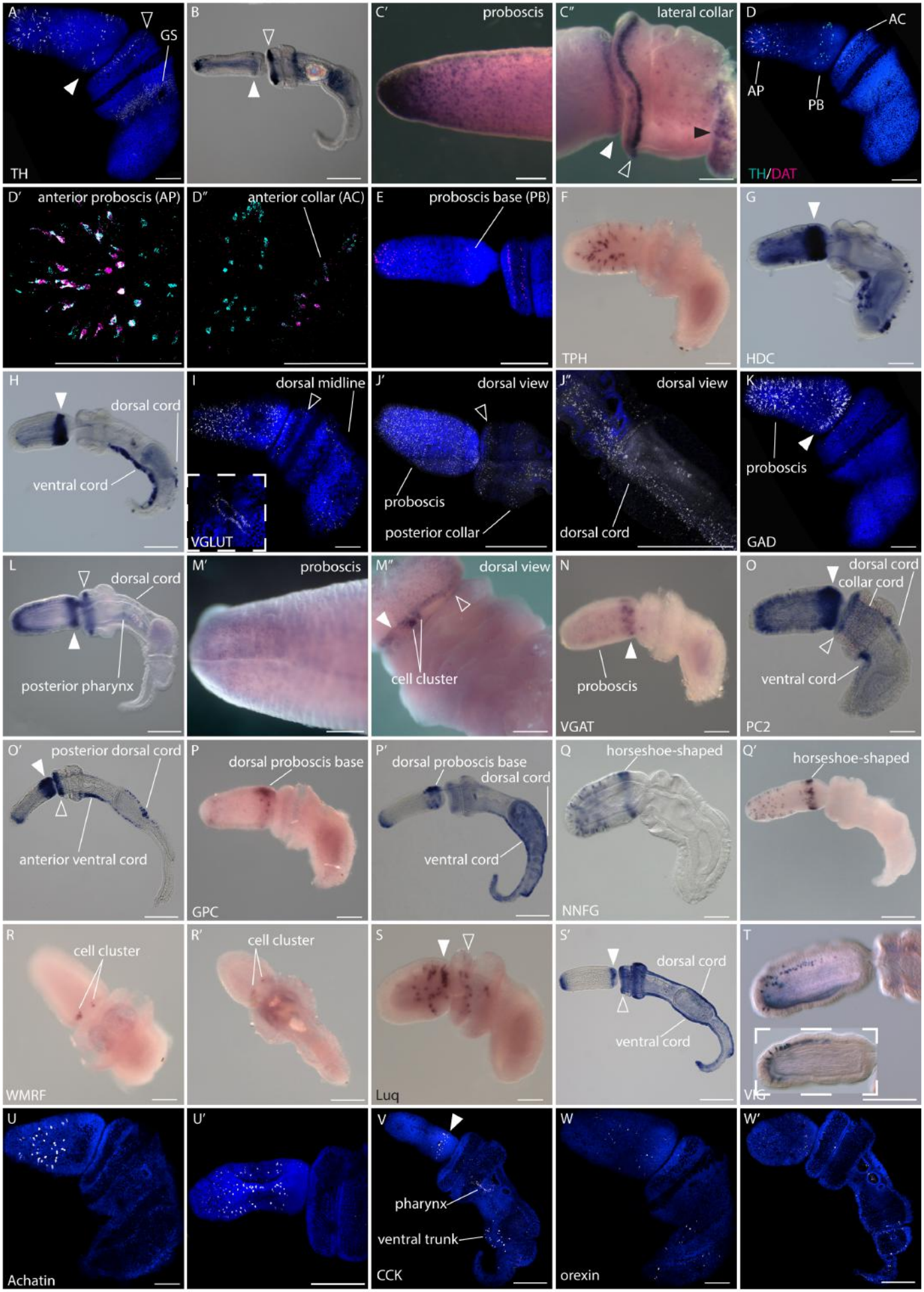

Scale
1GS: 100um
3GS: 200um
adults: 500um

Figure 3

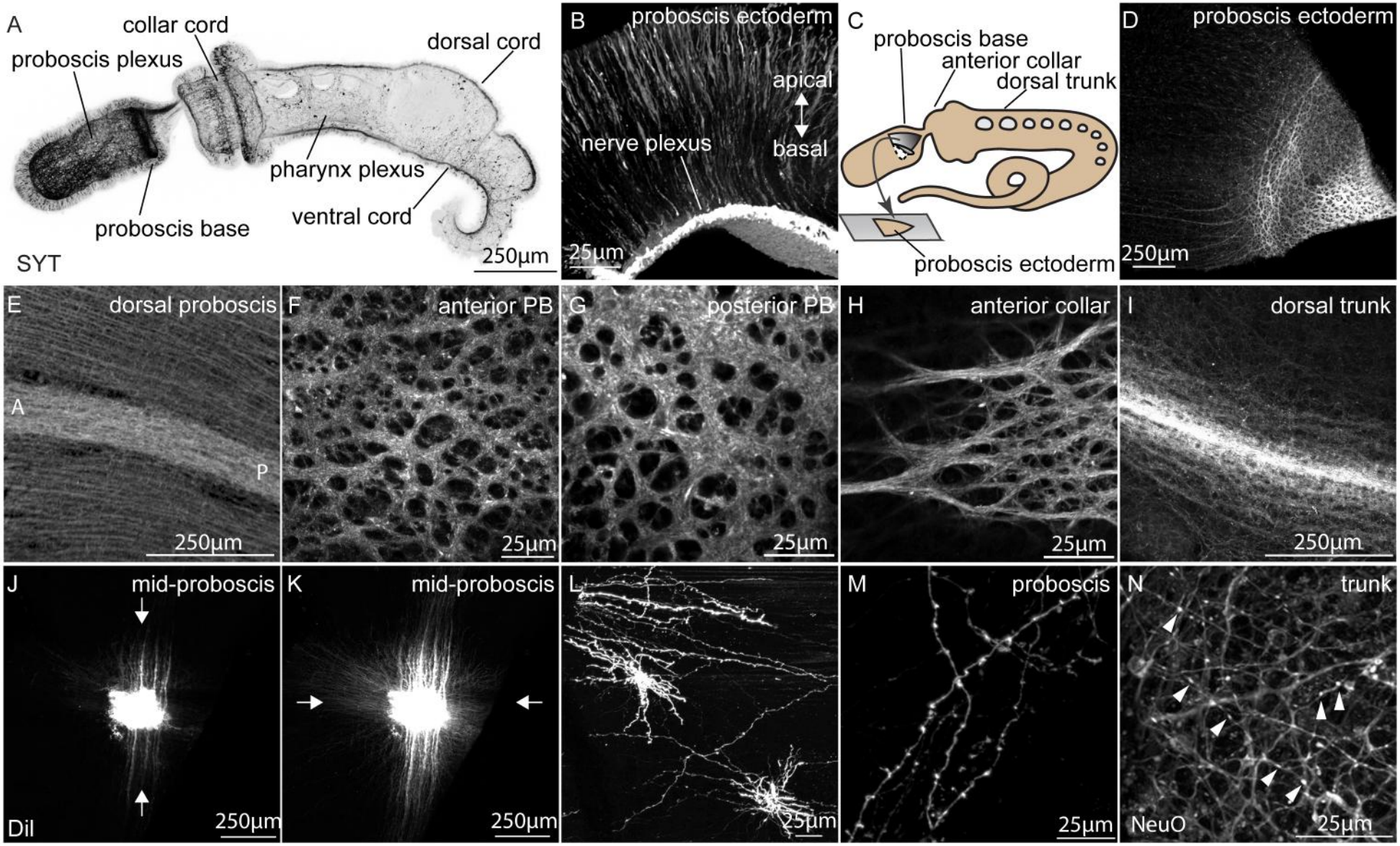
A
collar cord
proboscis plexus
dorsal cord
pharynx plexus
ventral cord
proboscis base
SYT
250µm
B
proboscis ectoderm
apical
basal
nerve plexus
25µm
C
proboscis base
anterior collar
dorsal trunk
proboscis ectoderm
D
proboscis ectoderm
250µm
E
dorsal proboscis
A
P
250µm
F
anterior PB
25µm
G
posterior PB
25µm
H
anterior collar
25µm
I
dorsal trunk
250µm
J
mid-proboscis
DiI
250µm
K
mid-proboscis
250µm
L
25µm
M
proboscis
25µm
N
trunk
NeuO
25µm

Figure 4

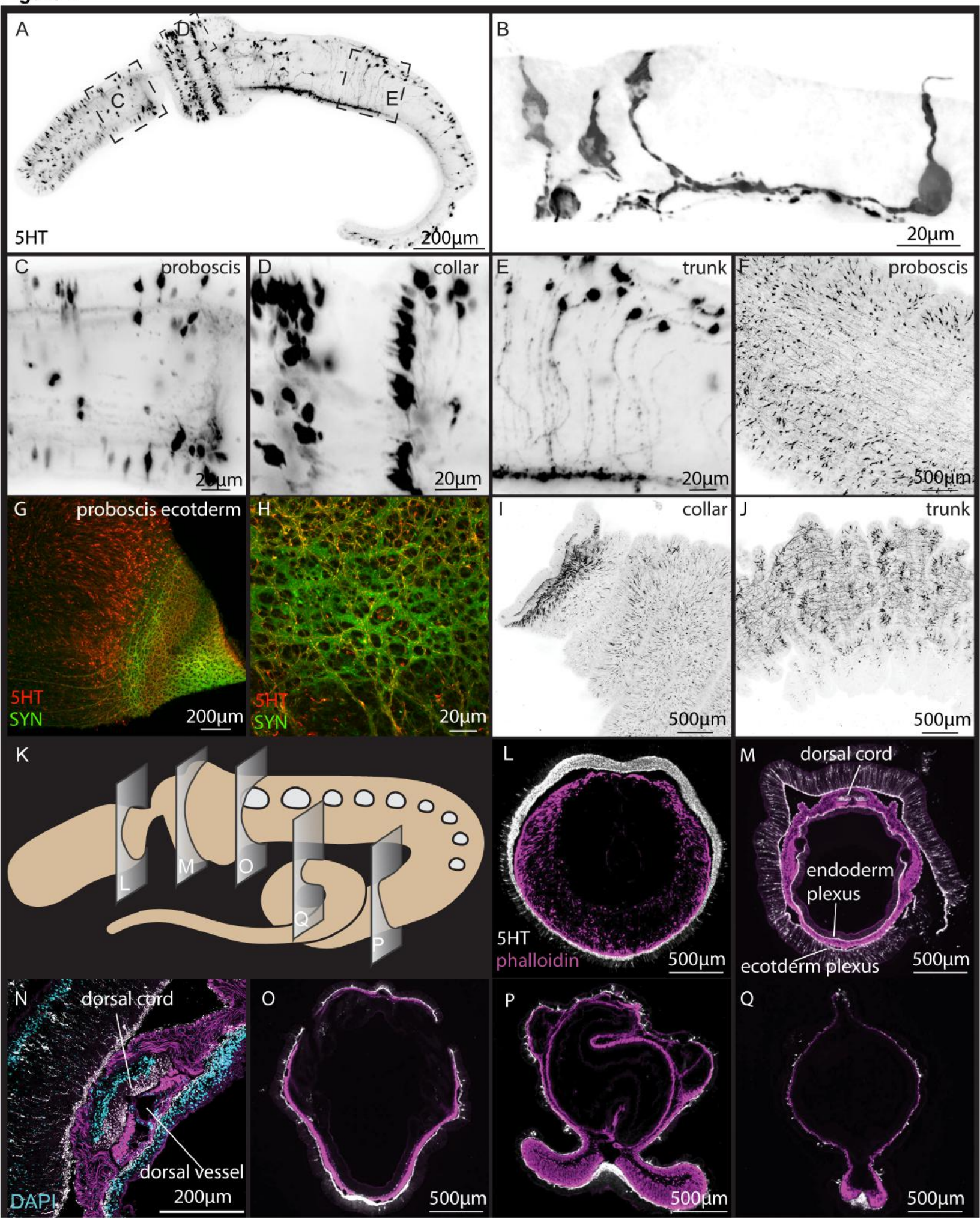
A
B
C
D
E
5HT
200µm
20µm
proboscis
collar
trunk
proboscis
20µm
20µm
20µm
500µm
G
proboscis ecotderm
H
I
collar
J
trunk
5HT
SYN
200µm
5HT
SYN
20µm
500µm
500µm
K
L
M
O
Q
P
L
5HT
phalloidin
500µm
M
dorsal cord
endoderm
plexus
ecotderm plexus
500µm
N
dorsal cord
dorsal vessel
DAPI
200µm
O
500µm
P
500µm
Q
500µm

Figure 5

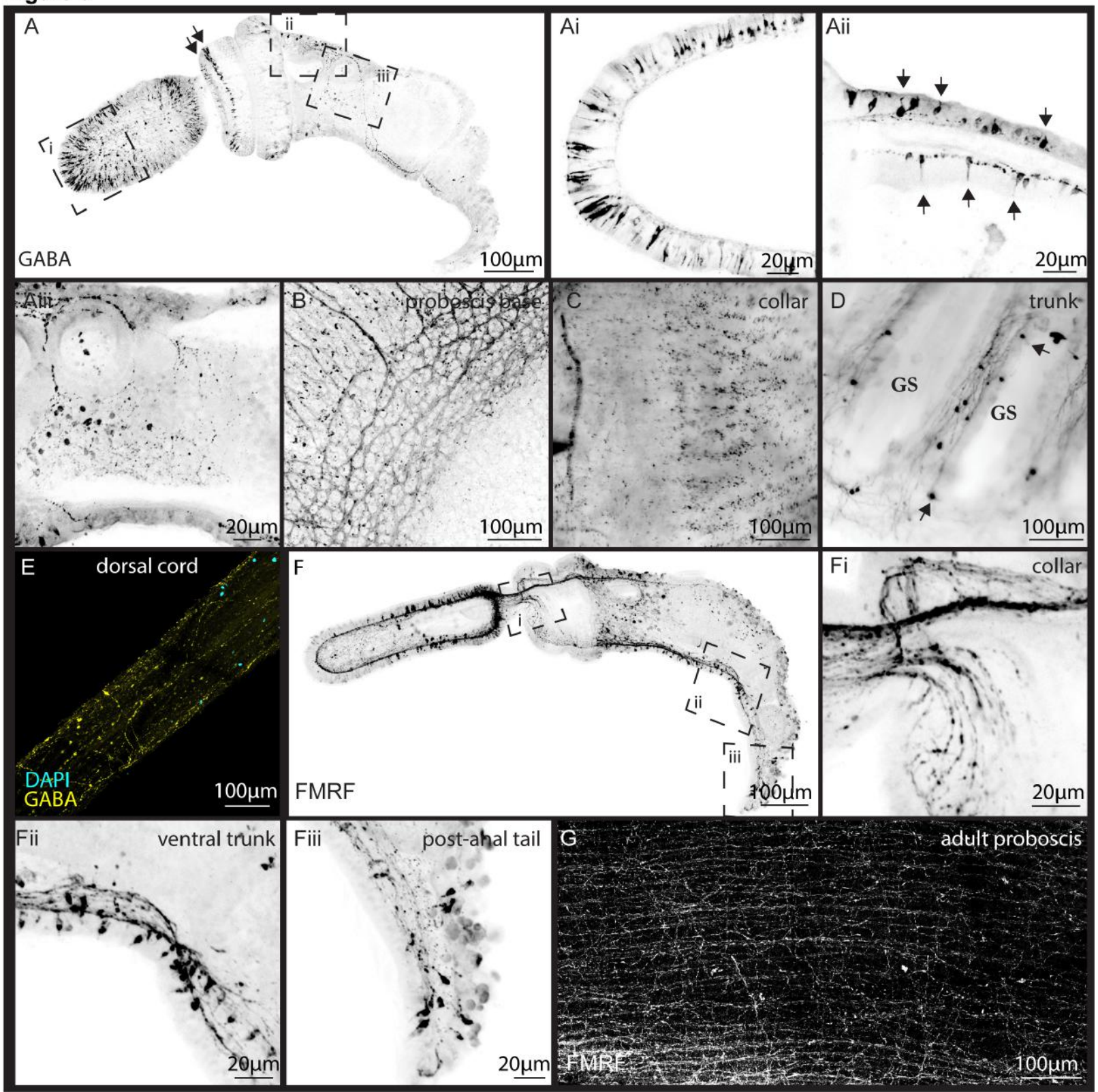
A
ii
iii
i
GABA
100µm
Ai
20µm
Aii
20µm
Aiii
20µm
B
proboscis base
100µm
C
collar
100µm
D
trunk
GS
GS
100µm
E
dorsal cord
DAPI
GABA
100µm
F
i
ii
iii
FMRF
100µm
Fi
collar
20µm
Fii
ventral trunk
20µm
Fiii
post-anal tail
20µm
G
adult proboscis
FMRF
100µm

Figure 6

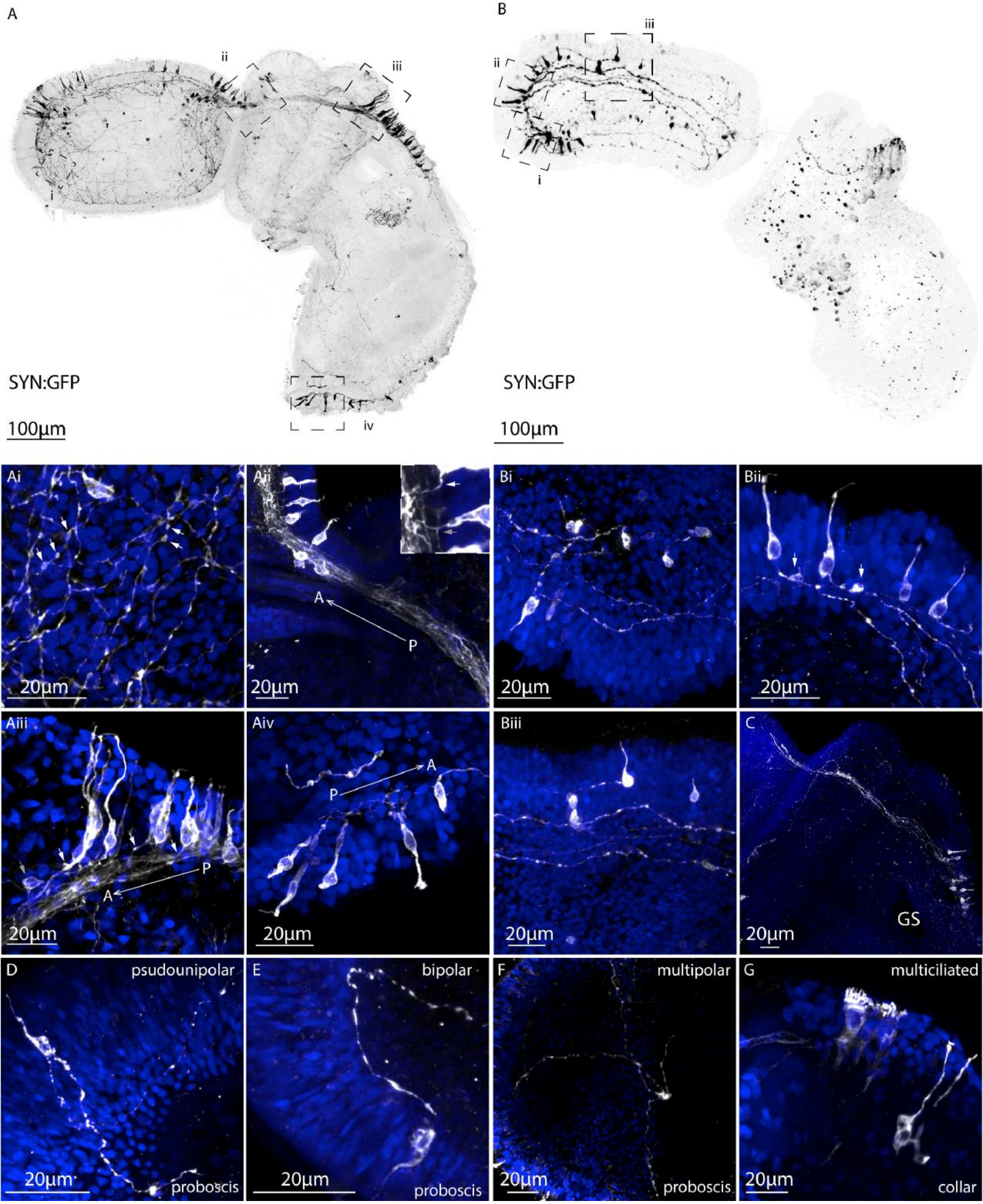
A
ii
iii
i
iv
SYN:GFP
100µm
B
iii
ii
i
SYN:GFP
100µm
Ai
20µm
Aii
A
P
20µm
Bi
20µm
Bii
20µm
Aiii
P
A
20µm
Aiv
A
P
20µm
Biii
20µm
C
GS
20µm
D
psudounipolar
20µm
proboscis
E
bipolar
20µm
proboscis
F
multipolar
20µm
proboscis
G
multiciliated
20µm
collar

Figure 7

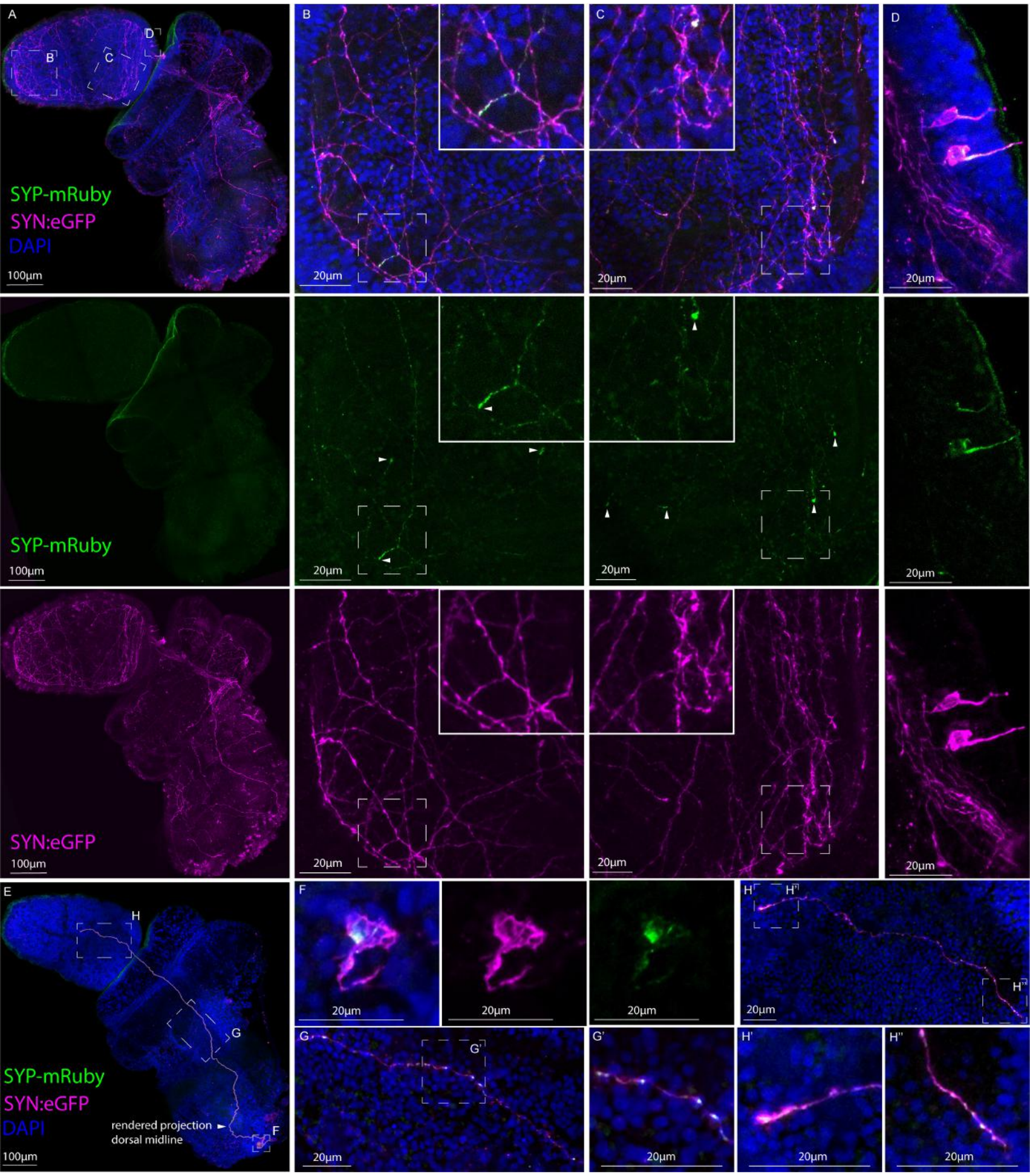
A
B
C
D
SYP-mRuby
SYN:eGFP
DAPI
100µm
20µm
SYP-mRuby
SYN:eGFP
E
H
G
F
rendered projection
dorsal midline
H'
H''
G'

Figure 8

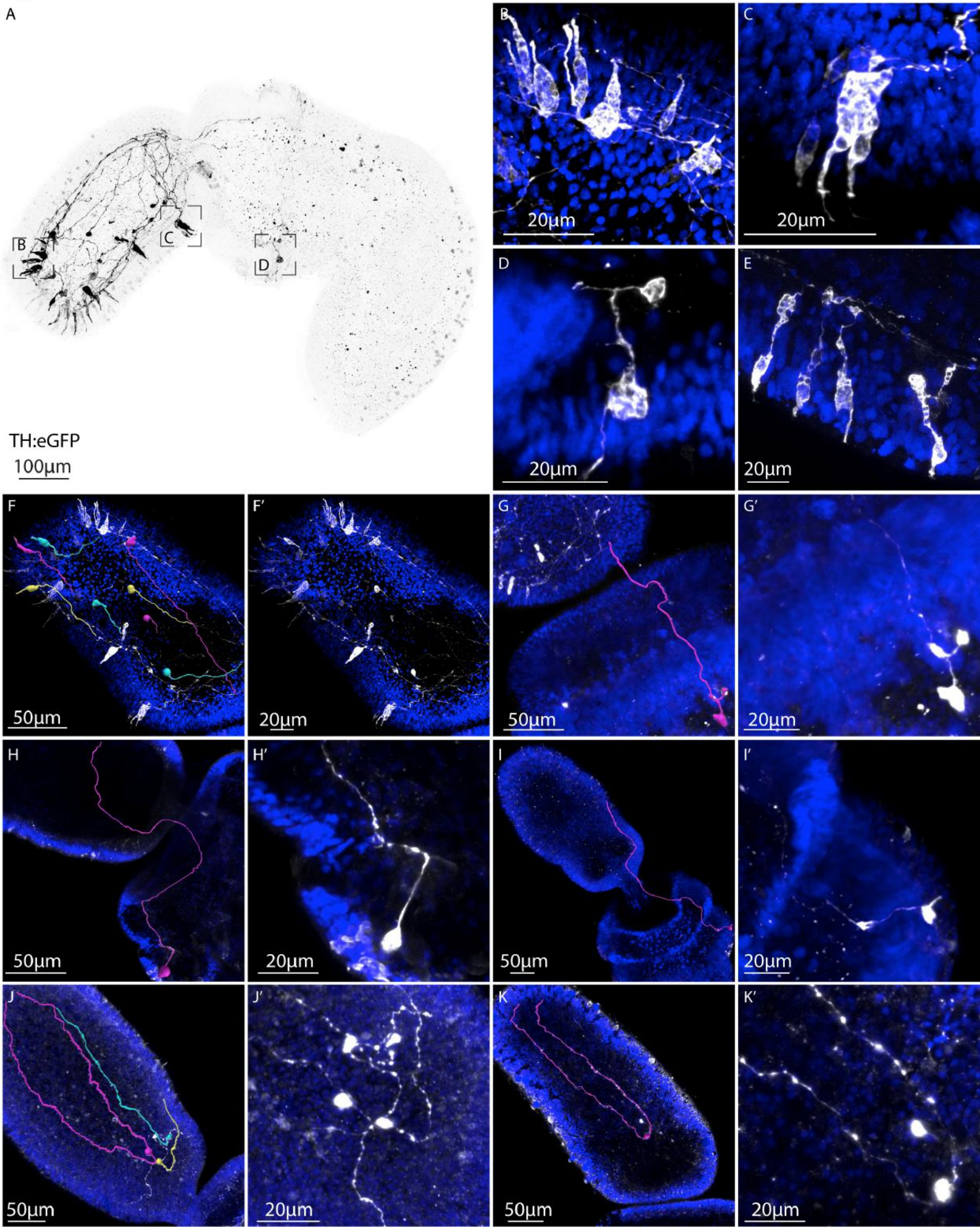
A
B
C
D
TH:eGFP
100µm
20µm
20µm
20µm
20µm
F
F′
G
G′
50µm
20µm
50µm
20µm
H
H′
I
I′
50µm
20µm
50µm
20µm
J
J′
K
K′
50µm
20µm
50µm
20µm

Supplimentary Table 1

Transgene name	Gene	Vector Backbone
TH:eGFP	TH (XM_006813504.1)	HCL
Synapsin:eGFP	Synapsin (XM_006820227.1)	HCL
Synapsin:mGFP--T2A--(mouse)Synaptophysin-mRuby	Synaptophysin (NM_009305.2)	Synapsin:eGFP

Primer Name	Sequence
flex_5prime	cgctttaattcaacctcaaaATGCTGTGCTGTATGAGAAGAACC
flex_3prime	gtccatgccgagagtgatccttACCCTCCGCCCAGGCCGGCGAACTT
flex_3prime-alt	gtccatgccgagagtgatccttCACCATCGACCCGAATTGCC
5UTRsynapsin_flex	TTTTGAGGTTGAATTAAAGCGGGTGA
HLC5primer_new	GGATCACTCTCGGCATGGAC
HLC5Prime	ATGGTGAGCAAGGGCGAG
HLC3Prime	CGAACCACTTTGTACAAGAAAGCTT
5utrTH	ctcgcccttgctcaccatTATACAGCCATAAAACTAATGTCAGG
5th	aagctttcttgtacaaagtggttcgCCAAGTGAGCGAGTGAAACG
5utrSynapsin	ctcgcccttgctcaccatTTTTGAGGTTGAATTAAAGCGGGTGA
8Synapsin	aagctttcttgtacaaagtggttcgACAGTACATGCAGTTAAGGTGTGG

HCR Gene	Asseccion #
TH	XM_006813504.1
GAD	XM_002740628
VGLUT3	XM_002739644
DAT	NM_001168055
orexin	XM_002734948.2
CCK	XM_002738068.2
achatin	XM_002732101.2

RNA *in situ* Gene	EST Access #
Achatin	G142P60143RF11
Cholecystokinin (CCK)	G826P5295RC10
Dopamine transporter (DAT)	G142P60116RF4
Glutamic Acid Decarboxylase (GAD)	G6027491317
GPC1	G826P5260RD11
GPC2	G613P6167RA7
GPC3	G178P60076RG2
Histidine Decarboxylase (HDC)	G142P60145RF11
Luqin (Luq)	G142P60091RF7
NNFG	G613P6343RF5
Orexin	G826P5320RC7
Prohormone Convertase 2 (PC2)	G826P59RB9
Tryptophan hydroxylase 2 (TPH)	G826P5282RG11
Tyrosine Hydroxlase (TH)	G613P6079RA4
Vesicular GABA Transporter 1 (VGAT1)	G142P60044RE10
VGlut1	G142P60093RF5
VGlut3	G142P60052RG5
VIG, IVG	G826P5251RB11
WMRF; WMRFamide	G826P521RB1

TH:eGFP sequence insert:

CCAAGTGAGCGAGTGAAACGTATGGCGATCACCTTTGGCCTTTCAGAAGGTTGCTATGCAGCTGCTTTA
GGAAATGCTTTGAAGATATTTGAGGTATGTATTATCCCCCAAAAATTATAGCGGGGGAGTCGTCACCTG
AGCATGCGTCAGATGGCCATAGCGTGTCATTGTTTACAAACAAGCGTCTACCCATGGGCCTTTGCGTTTT
TAGCGTGTGTTGCTATCGCCGCTTGGGGCTCAATTCCCGCGCGTGCGCAGGTGACGACCCTCCCGCTTTA
AACACATCGATACACAATCAAACATTTAACATCAGTTCAAATTTTATTGCCGGCAACATTTTGTTGAAAGC
CCTTTTATTTTGAATAACTTGGTCCAAGACGTTCTCCTATTCGTGTTTCGGTGATTTCATGACGCCAGAAG
ATATTGGACACTCATGAACAAATTCTACGGTCATTAATATCTGTTGCAATTGTGTATGACGTCACATTCCT
CAACGGGAATCGGGTCAAATATAGTTTTTTACGACTTTAACAAAGTGACTTTTTTAATTTTCTCAGCAGTT
AGAACCATTGCAATTTTTGATAAACAATTATGCCATTAGTGACTAAACGTGTAGTATGACGTGTTTAGCA
CCAACAAGTTTGCAGTGACGTCACGCGTAGTATGACGAGCCATGTCAAGAATGATACAAATCTGAGTAC
TTTGTGCCAAAATGTTTGCTCTGACGTCACGTGCACAGCGATGAGTCGTGCCACTGCTGCTGCAATTTTT
GCGGTAAACGACACACACTGTAACGTGTCACGCTTCAATCTTCCTGTGTATTGTAGACATTTCCCGAGGT
TCAAAGGTCATGTAACGTTTTCTGCTCTGCCTAAAATCGCATACGGCGGATATTTATTTTAACAAGAATTG
ATTTTCACTATGTGTTCTTAACCAAAACGTGCAAGTAACACAAATGCTAGCTAGAGAAAGAAAAACATAT
ACAGTTTCACTAATTATGTTTGCGTCAAACACCGCCCTTTCAATTCTCCGAATATCCGAGCTATTTATACA
GCGATGAATGTAGCTATTGTATTTTCATTTCCCGATTCGAATTGTGGAAAGACGTACATTGTTGCCTTGT
GCATTCACTGTAATTGACGAATCGTGGTCTACAATAATGATTCACCATGTTTAAGCGAAGTCCCCTGCGG
TCATTATGAGCAACGGGTAAACTAATTCAGATTTCCTTTTTAATTCTAGAATAATAACAATCCATTCTATA
CTTCACGTTTGAATAACATTGCATAGTGTTATCTTAATATAACATGGAAGCTCCAATATTGTCGAAAGTAC
CCAGGCTTACACAGCAACATCAACCACTACTCGTGATAGTTAAAGGGCGGTGGTTATCGCGCCGCGCAT
GTGCGACATTTGTGTTGATAAACATTGATTTTCCCATAATCCAATGCGCCTTACGTTACGGTGACAGATG
TATAATAGTAATTAATCAAAGATTTCTGCTTGCATATTCGCATAAGTTTTTGTTTTTTTGTTTTTGTTTTTTG
GATAACTAATCATTCATTTCACTCGATCATTGTTCATAATCCACTCGGGTTGAATTATTCTACAACTATTAC
TACTGATAAATATGCTGGTTTTTGCTACAAGTATAAACCACTTGGCACTTTTTTCGCCCATGTCTCTTGGC
GACCAAATTCTAATTGTTCGCTTTATGATATCACGAACTAATTTGTATAGCAGCCTACAATGGTCTAAATA
TTACTATTCTTTTGTATATTTTTCTTGGGAAATGAAGTTCAAATATTTGATCTTGTCTATTTGTACTCTAGT
GTAACAAACTGACTGGAGTTATATTTACTTTCGAACCCAACGTGTCACGTGGCACAGTCATCGTGAAGCG
CGTGTTCGAATTTCGTGAGCACGTGAACTCTTTACGTCACCTGGTGGTATATCACTTGAAAGCCGTGGTC
AAATTGGCCTACATTGTAATATGCAAATAACTTGTAAATAAGCCAATCAGCGCACATCCCTTCATACAGA
TAACCAATCAATCCACTTGAAAAAGCAGGCGATCCTTGCTCTAGTTTTAAACAAGCACTGATTGGTCATT
TGCTTTCATGACGTTTACTCATGATTACTCAAAACAATTCTCAAATATAGTCGAGAATGAGAATGCTTGA
AGCTTGAAGTAAAACATAACTAATACTCCGTAATCGCAACTTACAGTTACACTCAATGTAGATCATCGCC
AGGAGATGATGTCTTCACATCAGCGAACCGCCCCTTACAAGCATAGCTGTCCAACGCATAGTTATATTTA
AGTGGATACCTTTTAATAGGTTCAATATTTGTATAAACTGGCAAATGTTAAGAAAGATGGATGATATTAT
CAATCATATAATGAGTAATAGTGTAAATCACGGTTAATGTCCCCAGATTACCCACAAACCGAGTCAATAT
GGCCTGTGGTCATACAGAATAGACCATATGTAGTGCGGGTGTTTATGCCATAACATTTCGACAAACTAG
GCTCTAAATATCATACGGCATTTTACAGGTTAAATATGTTAAAAGGGCTGTCAGAAAATCCTACAGAAAA
CAAAATCTAGATACAGATAAAATAAAAGTCCAGCACGTGTTCGTATTCCGTGTAAATCAAAGATGCATTT
AGCACATTTAAACATGTCGAAGACGATTATTCGCAAAGACCATCACATTTAAATTAATTGTGGATAGCAC
ACTTAGAACACAGCGGCAAGTTCATCACGTAGTTGTTTGCCTGAAAATTATGCTATCCTGTCTCCATACTT
TCTCATTGCATGTATATACGCAACTGTTATTCCTTTCAACGGAAGTACATTTGTTACGGCACCAAACTGCT
TCACAGACCTGATATGTGGTGTCGGTACTTTGAAAATGAATTATATCTTTATTGAGCGAATTATCCTTGGT
TATTAAGGATTCTCCCATTTCAAAATAGTGGATTGACTGGAAGATGTTGCAGTGAAGAAAAAACAAATA

ACATGATTTTCAATTTCCATGACAACAACATAGCGTCGAATGTGAATAATAAAACTGACGTCAGCCATGG
GTGAATAAATATTTTCTAAATTCCACCATCCCCACTACCCACCCTGTAATCTCCTACAACGGAACCCCGCG
TATAGACAGGCTCATGACGTGCAATGTGGTTATAATGTAAATCTAAGAGAAACTGGAAAATCACCCTGG
TGTATAATAATAGGTCTTCAGGTGGAATTATCGGCTTATATGCGAATTTCCGATTACATCATTCATGGTAT
CCGCACGTGCCAGAACTACGTTTGCGCGGATTTGACAGGCATCTACAATGAAGAAATACTGTGAATCGA
GCCCAGTTCTGTTCCATTTCAAAAATCCCTACATAGAAGTTATGTGTTGGATTCCAAAATCGTATGTTTGC
CGGTTGTTTCCATGGCAGCGTCAATCAAAAAAGTCCCGCACGTGGGTCAATGTATGTCTGTGCTATTTAG
TTGGCTGTTAAGTAAAACAAACTGAGGAGAACACCGTGTGTATAACTGAAACCAACAAATATTGGCTTTT
TACGGAACTAGGGGGGTTCATATGATAGACGATATGACCATCTGTCTAATGTCAATCTAATACTGCATCT
GAATCAATGTTTACAAGACATTCATTCATGATAGTGTAAAGGATACATAGAGTAAGAGACGGGAGTACC
TAGTACATGGTATCAGTGCTACGTCGCAAGCGAGGTCAAAACTGGCGTATACCTTGAACAACCTTATATA
TTGGCCCTACATAGACGAGGTCAAGATGAAAAGTAATCCACAGTCATTTTTTTTCACGATTCCACGCAAG
ACTGGTTTTGTTTCGGTGTCACTTCCTGATTTACGTGGAGTTTCTCGTGATAGTGCATACGAGTGATAACT
TAAGTGTAGAAAATCGGGGATAATTACAGCTCAATGCAATCAGAAAACTGAATAATAGGCCACTTTTAA
TTCCATACATATAACCTATATTTAATTCACATTTATTCGAATGTATTATGATAAAATAAAGTTTATACTTTC
ATTTAAATCACTGTATTATAAGTTTACCATGATATGTTGCTAATTAATGGGTTGGGATGAATGCTTAGTAT
CTAGCGTTTACACCAGCTCAGTGAAAAGTCGGCGATTCACGGGCTCTCGCTTGGTCATGCGCGAGATAT
GCGCCTATAGCAACAAAGATGGCGACTTCGAGTATTTCGCGGATCAGCGGATACAAAAAAGATACGCTA
CCAATGTAATTCTTAGAATGATTATGACGTATATCAAAGAATATTTCAAAGTCCAAGTCGATATTCAGTG
CACATGACACGCAGATCAAAACTCGCGTTCGTGCTTTTCACCCTGGGAGCGCACTGTATTATGGGAATCT
CAACGTACTGTATATCTCGCACATGCGTGGCACGAAGACTACCGCCTTTTAGTAAACAGTTACAGCGTCA
CGACAGTCGCCGTAAAGCGCGTTCGAATTTCTTGTAATATAAATGTGCTGCAACAACTTAGGCTTTTAAG
TAGGAAGTCCATATTTGTAGTGTTAGGCAGTTGTAGAACTTCATTTCCTTGAATCAATCATACAAAACATT
GTTTGATTAGCGCAGCCTTGACGCCAATTTGTGGCATACCGTGCTCCACGAGGCTTTTAGTGTCAATTGT
TTCCTTAATATTTTTTGCCTTTGATTCTTACCTTGAGGGTTTCTTCAGATTGGAACGTGCTGAAAGACAGC
TACTTTATTATATACTCTTTATTTATGAACGTTTAGTGACGACCTAGAAAAGAGCTGTAAGGGTTTTTGAG
AAATGTGATCATAGAGCATCACGTGACGGAAGTGGAAATATGCCATTTGTAGCTCATTAATGACAAGGA
TATTTCTAATTCGGCTCACAATTTTGTTGATTATTACGCAGACTAATATAGGGCGAAAGCAACATGTTGA
ACAGAGTGTGTCCATTCTTTTCGACTGACACCTGACATTAGTTTTATGGCTGTATA

Synapsin:eGFP sequence insert:

ACAGTACATGCAGTTAAGGTGTGGCCTTATGCTAGCAGTCATTTCTTAGACATTATTCACGATATGGGCT
TGACATTTTAACTACATTTGTATCAAGATAATGAAGAAAAACCTTTTTAATTTTTTTTTATATTGTCATTAA
AGCTGAAACAATAACATTTAAGAACAGCCATTGGGAGAATGTATAATAATTTTGAATTGTTGGTATGTAT
ATTAGGCTTGGTGTCTGTTCTGTTTTAAAAAATATTTAATATTAAAAATATGAGAAGACTCATACGACTG
ATAAATATAATGGTAGTAGGAAATCTTAATCTTACCAATTTCTATTATAGATTACACTTAGAATATTAATG
TTTTTAACTAGATTATAATAATGAATAATGTTATTATAATTAGTCATAATGTATATGAATATAAACTTAACT
CCTGAGAGATTTTCATAATAAATAATCAATTGATCGATTTGGAGTTTAATTTGTTTTCAATTATCACAAAT
GTTTTAAAGGAAACTTAATATTACTTTGTCCTTATTTCAAAAAAAGTGAAAGTTACTGAAATGTTCAGTTG
TGATGTATGGGCGCTATTGAATCAGTCATGCACAACATCTGTCACATGTAATTACTCTCTCATTAGTACAA
GCACACCTGCTGGCTTTGAGGTCATTTCCCATCATGCAACAGTTCACTATATGATCTTAAGGTGTGTATAT
CTTGCTATAAAAAGAACAAAAGAGTGATTTTTAAGTTGTGCTATACATTACCAAACCACACCGAATATAA
ACTTTCGTTTATAAAGTAATAACCAATTACGATGTGTTGATGATAAATTACTGCTACGAGACGAGTCTGT
CCCATGGGAAACAGAATATGTACAAGAAACATGTAGCACTGACCTAGAGTTCACTATTGTATGGATTAG

AATAAACTTTAACAATGCTTGGTTCATTATTAGCAGTTGCAGGTGAGTTAAGATGGATATAATATCTTTA
CTTGAAAGAAGGGTTTATTAATTAAGGCCTTTAATGCTGTTCCAAAATGTTGTCACCATAGGTCTGCAAC
TTGTATATAGTATATGTTCAAAGTTGAGAGTTTATTAGCAAGCAAATTGAACGTAAGGTTATTCAGTTCA
CATGTATTAATCTGAAAGGTGCATTATTTACTTGTACATTGACTGTAAAAATGTGTCTAGAATTTGTTAGT
TATTTTCAGAAATTCACAGAAAATTAGTGTTTTATTAGTGTTAGTTTTTCACATTTTGTCACTAATCCTTCA
GCACAAGATGTTCTACTTGTAATGCCTTTGGGAAATCTCCAAACCGACCGTTCTAAATGTGAGCAATGAA
GTTCTAAATGATACACATGAAAAACCTTTAAATCTATGTTTTAGACTTAGCTGTATAGAATCTGATCTCCA
CATGCCCATTTTTGGGGCAAAATTTAAGTGCCTCAGAAATTGGTCAAAGCTCCAGAGGGAAAGAATCTT
GTTTCATATAAGGGGATTTTGTCAATTTCATGTGTTTCTTCATTGTGTGCTACTGTGTCACAGACTAATAA
TAAGACATATTAATACCTACTATCGTTAATCTTTGAATAAAAAAAAATGATCAAATGAAAGTGATTTTGA
AAGTTGACAATGTCAGGGAAAGGGTCACTCTTATTGATAATTAATTTTGCAAAAGGAAGCAATTGTGAA
TTGGAAAATGGCAAAATGATGTAGCAGTGAAATTTAACGATGTACAGTATAATTAGAATTTTTTTGATAT
TCTTTATTTATTGCATTGATGTCAAAATACCATTGAGGTGGTGAACAAGGCCTTTGAGGTCTCAATACAA
AATTTGATTTTGTGCATTTTCAGTAAACTGGGGAATTGTATTTGCATTAAAACATTGAGAAAATGAATTAT
TCATGTTAAGTTTCCTGGCATGTTATTTTTATTTCAGAATAAATAATGCAACAGACATATCAAGCAAATAT
GCTTGATATAACTGAGGCTTAAAATCCAATATGCATTTTAAATATTAAATTTGCAATTCATTCACAAGCAT
AGGAAAATATACATGATAATTAATGTGTAAGATTGTATTATAGGATTACAAATTGAAGACTTGATTTTTA
GCATTGTTTTTGCACTCTTGCTTCATTTTTGAAAATAACTCCCCTGTTATTGGGCCCCATCAAATAATTATC
TCAAAATGAATTTCATATATTACGTTAATTCACACCACATACAATGAAATATATTAAGTGCCGGTACACTG
CCAGCGGTTCTCAACTTTGTTTTGTTCAACTATATACTATATAGTATATATTGCAATTTGATTGTAAGGTTT
CCTGCAGAATCCAACATGATGAATCAATTAATATACACTTCACTTCAATGCAGGTACTGTACATTAAATTG
ACAGTACATGCTTTCCCGTTGACTCAAATGTGATGCATGATTTAGAATAGGAACATCCAGGGTATTTTGA
GGTCTAATGAAGTGACCTTTATTTGAGCTGAAATTGCTAAAAAATGTATTTTGGCTGTTTTGTATGGCATT
TATTTTAACTGAATTTTGATGAGTTGAATGTAGAACACAGGGAAAAAATGTGTTCACTAATTCATCCCTTC
AGCGAAAATAGCAAAAATAAATTCCAATTATTAATAATAAAGTATTTTACATTCTGGAGAGCTACCTAGA
AACATAACATAATACTGGAAGTGCATTAAATATTCACTGGGTTTTAGTTATTAAGTTCATTGTTATTTTTG
CTGATGAGTAAAACCCGCTAAAAAATTCACATGGACTTGTAAAATTACAATAGAACTCATTATTTTGCTG
GTAATTCTGCGAATTTAAAATTCAGTCAATATTCAAAATGTACAAATAGTGAAATTAAATGCCAGCAAAA
ATATATGGTTTTACGAGACTAAGTAACTTAATTGAAATATGTACTTTTGTACCCTTGTGCAACTATCATGT
TTTATATTATTGCAACACTTATATCATTTAAACTTATAAGTAAATTGGAAAGAATATGAATATATGAGTAG
AGGTCGATGCGATTGTCTACTGTCTGACTGCATACTTCAGGGTATCCTTGTGATAACCTTATTTTCACTGA
CTTACGAAATTAAATCAGCTTTCAGCATATTCACACTTTGTGATAGAAACAAGAAGGCTAGTGTAGCTGT
CTCAATCAGTGTATTCTCCACCCACACAGATTTCTCTTAATTTATTGAATAAATAGGAATAGTGAGTGGTG
TTAACTAAATACACTGATGAGATTTCTTCCCCCAATGGGATTATATACAGTTGCACCAGTGAATGCAAAA
CTGTTTCATTTAAAAAAAAAATTGCTAGATTACATATATTTCATATATTAGCTGACAAGTATTTTTTACACT
ACTGTGAAATACTTTATTTTAGCTGGAATTAATTTTCGCTGAATAGACTTTTTGGGTGTTTTGTATGGAAT
TTATTTTCACTGATTTTGATGAGTTCAGTGTAAAATATAAGAAAAAAGGTCTATTCACTGAATTTTATTTT
CACTGAATCCTTCACCAAAAATAGTGAAAATCAATTCTAAGCGAAAATTAAGTATTCTATAGTACCGGTA
TATTGTATTATTTTTCAAACCACTTACATACAATTGTTATCCCTTGAGTTATCAGAGGCCTGCTGTTACCAG
TAAGAGCAGCATTTGTGGTCATGTGACTGTGATTATGATATCCATCTACTGTGTCCTGGACAATTTTAGG
TTGGCTGTCATTGAATGAATCTAATTATGCATAAAATCAATCAATAGTTTCACGACTTTGCTTATCAATTG
AGCGCTAAATTCTTCCATTTAACGGGTCTTAGGTCTTTATGTATAATTGTGTGTTCATAAAAGAATGATGC
TAGGCTTTATGTGTGACAATTATTGCTCACATAAAGAAAAACTACCATTATCATAATTTTACTAATACTGA
AGCCCAAGCCCTGGTGTATATTGTTCAATGTATTCCTAGATAAACTACATGTATATTTGTTGACTGTTATT

AAGCGTACCAAAATATGTTTTTATGCTTACCTCATCAGATTTCAATGAAATTTTGTGCACTGGGTGATATG
GGGATAACTGAGTGACCAAAATAGTTCTTTCTTTTAATCTATGCATATTAATTATCTAATTTGTCTAATAAT
ATTACCTCAAATTTATATTCAATGGATGTTCTCATTAGACTATAAAGGAATTCATTAGAGACTGGGATTTA
TGTGATGTGTGATTTTTAACATCAAATCTTTGCAAAGTAATTAGTAAACACTGTTTTTTTATAGAAATATA
TTTATTATGAACTACTTGTAGCTAATATGCTAATTTAAGTTATCAAACTAATAAAAGTTAAATATTTTATTT
TACCTTCAACAAGCTAATTTTCACCTTTGTAATATCTAGTAAATGAATTAATTGTATTTAGAATTCAATTTA
ACCCTATTAGAATAGTAGTATATATTCGTCCATTACAAAATAGTCGAGCCAATATAGTTTCAAAATGTTAT
AGCAGATTGATGATTCTTGATAATATTGAGGTCAGTACATGGTAAAATATTTGCCATCTCTAGATTTCTCC
ATTTTGTAAAATCTTGATGACAAAAATTGGATTTATTGATAATCATCTAATTTGATCTTTATCTTGTGTCTT
GTTGTAATGAGTTTGTTATTACCGGCTCACAATTGATGTGTATGTGTCATCTCTGAAAGTCACAAATACTG
ATACTTTTTGGCATATTGATGCTCTATAAAAATACTTTCACCTGGAACTATTTTCCTATATTTTACATCAAA
AATCAGTGAAAATAAACTTCATACAAAACTGTCAAAGTGTTATTTTCAATGAAAAATAAAATATTTTACAC
TACTTCAATTTTTGCCATGTACTGTTTTTGAATTTTTATGATTACTGCTTTGGGGAAAATAATTGAAAAATT
CTCATTTGACCTTGGTGGACTTTGTATTTTGGATTCCATCCCTGCAAATCATAATGGGATATCCATATGCA
CATCAATTTGTTTGGTTGACGTGTGGCTGACTGTCAGCCATTTTGTCCCAAATTACATCTAAACTGTTTCT
CGGGCATACCTGGACTGATTTCATTGTGCCATTGACATTGGTATTTTTTATGTAAGTCAATTGGTTCACAA
TTTGATGCATTATTTTTGTTATAAGTGATACACTTTCACAGATTTGTTTAATTTTGGTACAAACACAAGTCT
TAATTGGTTGCATGAATTGGTTTAGTTTTTTAAATAGTGAAATTACATACATACTGTGCCAAGTAAGTTTG
TCTTTCTCCCATTCTGCCCAATCACTGTCAAAATTCAGTAGCACGTACACCTCCCTAAACTGCCAGTCAGT
TGATAAATATTAATTAGTAAGTGCATTTTTGTACCCTATTTGCATTTTAATTGTGAATCAATCCTTTTATGG
GCATGCCGGTAATGACTTCCCTGTTTAGGTCATAAGAGATTATTTTTAAAAAAGTACCAACATAGACTCT
GTCATTTTCAATGACTTGATAGTGAATTAATTGTACTTTCAGAGAGTACCAGAATGTGTGATCTTTCGGA
GATCATGCATGAGTACTATTGCCCACTCGGTCTGTATGGCATTGCGTTTCTTCCCAATAATCAAACACAG
GTAGAGATGTCACTTCATTCTCAATTTAAAGGTTAACATGGTAGTGCTTAATTGGCATCACATCTCATGG
GATTTAATTATTATCTATGAGTGTTCAATAGTTACAGTGTATGTGAACTGTGTGAAAATGTGACTGATCA
GTTTATTCAATGTCTATAATATAAATGGTGCAACAGTAATGTAATACTGATTTATCACTGAGTAAAGGAT
TCAAATCACAAAAAATTTGTGTCTCTTACTTTTAAATCACAAATTTTGATTAGCTCCACTGTCGACTTTGTC
GAGCGGAGCTTATCATATGAGTGATTGTCCGTCGTCATCTGTGGCAATGTTTTACTTTTTCGACTTGAAA
ACTACTAGCCTGAATGCTTTGATACTTGGTGTATATGTACCTTGGGTAGACCTCTCTTAGGTTTGTTCATT
TCATGTTGATATCTTCAATTCTCTAATTTTGGTGTTTTGTTAAAAACCTCAAGTCTAATTGCTTTGATATTA
TATATATAAGTACTACATGTGGACTCTCTTTCAGATTTGTTAATTTCGTGGTGATATTTTCAATTAGCTAAT
TTTGATGAGTATTTTTGTCATTGTTGGTGAAAAGTGATATTTTTGACTTCTTGTTGAAAACAGCAAGTCCC
ATTGCTTTGATACTATACATATTGTTTATTTTCTAATGACATCTTCTGTTCTTTAATTGAAATGTGCCTTGCT
AACAGCAGAGCTATCTCGGCCGACCTGCTGCTTGTTTTGAATATACATTCTGTAAATATCAGATACTGTTT
TCATATTTGTTTATTTAATATTTATAATAAATGCAAATTAATTATCCTCATTGAGACATGTTCTTGAAAATT
ATTATTATAGTTTTTTGGTATTCAATGTTGAGATACAACCTTGGCATTTACATTAAATAATTGATTAAATA
GCAAAGAGGTCAGTAAGTTATTATGAATGGAACATTTCATATTAACTCCATTAAAGGAAATATTGATTGC
TATTTTCAGCAAGTCAGAATATATTATCATAAAGGTATTGAAAATTTAAATATTAAAATGCACTAATAACG
TTCATTATTCCATATTCTATTGCCAAAATTTCTAATCAGAATTGGATGGAACAGTCAAACAGAAGTAATAT
AGACAGCAGTAAATGCACTCTGCTTAACAATTTGTTTTGCCTAAGGTCTGCAAAACACATATTTACTGTTG
AAGCTCATTATAATACGTCTGATTTATTTTCTGATATGATCCAGGTTTTTGAATAGTTCAATTTATGAAAG
ATAATCACTTCATTATTTCAGTGCTTTATTGCATCTCAATATGAATAAATTGAATTTTTATTTCTAAGGGAT
TGGAGAAATACTTCACTCCAGATGCTACTAGATTATTCTTACTTCTGAATCACTTTGGAGACTGTCAGTAT
GAATTTGAAATTCTTGTGATATTTATATATCATAATAGTCATTAATATTTCAATATACAGTATACTTTATAT

TCAGATATATGAAGGATATATTTTTTATTACTGATAATAATAGAATGCCATGTCCTCGACTTGAGGTTTGT
GGGATATGGAAATTATTTTCATGAGTGATTTGGATATCCTGCAGCAATATTTTCGCAAACAGAGTGAGTG
AAAATACAGCATGTATGCACCACATTACATATCTAATAGTATGACAGATAGTATATTTGTTAGTATTTTCA
CAAGTTATGCTGTAAGTGTAAAAAGTGAAAATAAAGCAATGGATTCACTGCAACACTTTCAAAATATAAT
TTTTTAGTGAGTATCTTTGAGTATTTTTAAATTATTAATGTTTGAGAAGATTACAGTGTATGTGAGGCGTG
ATAAATTTGGAATGGTACAAATGCTATATTCTATGCTAAAGTTTATTTTATCTAGTTGTCTGAATTGTGAC
ACCTTTGATAATCACTTCAAGTAAATCATTCCAGAAATACCGTAAAATAATATATTTTGTCTTTTTCACATA
CTCACTCACTTACATTTCTTTTTTTTTTCCAGACAAATGAAGTGTGTATGCTAGAAGATTGGATTCTTATCT
GAGTGATTCTAGGAATATTAATACCTAATGGAAACAATAGATTTTGTGTGATTCTACAGTATATAGAAGA
TTCAACAATAATTATTCAGCCAATCATCAGGGACCTAATTTACGCTTGGATGTACTGGTTTACAGATAAA
ACTGAAGTTGCGATACGATATAATCCTATATTTTTTTCATAGTAAGGTGATATTATTTTATAGTTGCGAAT
AAATATTTGAACTCTATTGCACCTGCTGTCGAGAGAGCTGGTTTTCTTATTTTTATGTGGCTTTGGTACAG
TTGATTTATACTCAGTAACCACAAGAACTTCAGCAATAATTTGATCCGTAGACAGTTTGTCTGCCGAGTG
TAGTCTTATTCCGTACTTGCTATTACATATTGGCCAGCTGTCAAAGAGGATATTACAATTGCGGGTCTACC
TCGTATAGTGAAATTCAATTCAACGCTGGCTTCTTATTGAACTAAAATCACCCGCTTTAATTCAACCTCAA
AA

<u>(mouse)Synaptophysin sequence insert:</u>

ATGCTGTGCTGTATGAGAAGAACCAAACAGGTTGAAAAGAATGATGAGGACCAAAAGATCATGGTGAG
CAAGGGCGAGGAGCTGTTCACCGGGGTGGTGCCCATCCTGGTCGAGCTGGACGGCGACGTAAACGGCC
ACAAGTTCAGCGTGTCCGGCGAGGGCGAGGGCGATGCCACCTACGGCAAGCTGACCCTGAAGTTCATC
TGCACCACCGGCAAGCTGCCCGTGCCCTGGCCCACCCTCGTGACCACCCTGACCTACGGCGTGCAGTGC
TTCAGCCGCTACCCCGACCACATGAAGCAGCACGACTTCTTCAAGTCCGCCATGCCCGAAGGCTACGTCC
AGGAGCGCACCATCTTCTTCAAGGACGACGGCAACTACAAGACCCGCGCCGAGGTGAAGTTCGAGGGC
GACACCCTGGTGAACCGCATCGAGCTGAAGGGCATCGACTTCAAGGAGGACGGCAACATCCTGGGGCA
CAAGCTGGAGTACAACTACAACAGCCACAACGTCTATATCATGGCCGACAAGCAGAAGAACGGCATCAA
GGTGAACTTCAAGATCCGCCACAACATCGAGGACGGCAGCGTGCAGCTCGCCGACCACTACCAGCAGA
ACACCCCCATCGGCGACGGCCCCGTGCTGCTGCCCGACAACCACTACCTGAGCACCCAGTCCGCCCTGA
GCAAAGACCCCAACGAGAAGCGCGATCACATGGTCCTGCTGGAGTTCGTGACCGCCGCCGGGATCACT
CTCGGCATGGACGAGCTGTACAAGGAGGGCAGGGGCAGCCTGCTGACCTGCGGCGACGTGGAGGAGA
ACCCCGGCCCCATGGACGTGGTGAATCAGCTGGTGGCTGGGGGTCAGTTCCGGGTGGTCAAGGAGCCC
CTTGGCTTCGTGAAGGTGCTGCAGTGGGTCTTTGCCATCTTCGCCTTTGCTACGTGCGGCAGCTACACCG
GAGAGCTTCGGCTGAGCGTGGAGTGTGCCAACAAGACGGAGAGTGCCCTCAACATCGAAGTCGAATTT
GAGTACCCATTCAGGCTGCACCAAGTGTACTTTGATGCACCCTCCTGCGTTAAAGGGGGCACTACCAAG
ATCTTCCTAGTTGGTGACTACTCCTCCTCGGCTGAATTCTTTGTCACCGTGGCTGTGTTTGCCTTCCTCTAC
TCCATGGGGGCCCTGGCCACCTACATCTTCCTGCAGAACAAGTACCGAGAGAACAACAAAGGGCCAATG
ATGGACTTCCTGGCCACAGCAGTGTTCGCTTTCATGTGGCTAGTTAGCTCATCCGCCTGGGCCAAAGGCC
TGTCCGATGTGAAGATGGCCACTGACCCAGAGAACATTATCAAGGAGATGCCTATGTGCCGCCAGACAG
GAAACACATGCAAGGAACTGAGGGACCCTGTGACTTCAGGACTCAACACCTCGGTGGTGTTTGGCTTCC
TGAACCTGGTGCTCTGGGTTGGCAACCTATGGTTCGTGTTCAAGGAGACAGGCTGGGCCGCCCCATTCA
TGCGCGCACCTCCAGGCGCCCCAGAAAAGCAACCAGCTCCTGGCGATGCCTACGGCGATGCGGGCTAT
GGGCAGGGCCCCGGAGGCTATGGGCCCCAGGACTCCTACGGGCCTCAGGGTGGTTATCAACCCGATTA
CGGGCAGCCAGCCAGCGGCGGTGGCGGTGGCTACGGGCCTCAGGGCGACTATGGGCAGCAAGGCTAC
GGCCAACAGGGTGCGCCCACCTCCTTCTCCAATCAGATGTCGGATCCACCGGTCGCCACCCGTACGATG

AACAGCCTGATCAAAGAAAACATGCGGATGAAGGTGGTGCTGGAAGGCAGCGTGAACGGCCACCAGTT
CAAGTGCACCGGCGAGGGCGAGGGCAACCCCTACATGGGCACCCAGACCATGCGGATCAAAGTGATCG
AGGGCGGACCTCTGCCCTTCGCCTTCGACATCCTGGCCACATCCTTCATGTACGGCAGCCGGACCTTCAT
CAAGTACCCCAAGGGCATCCCCGATTTCTTCAAGCAGAGCTTCCCCGAGGGCTTCACCTGGGAGAGAGT
GACCAGATACGAGGACGGCGGCGTGATCACCGTGATGCAGGACACCAGCCTGGAAGATGGCTGCCTG
GTGTACCATGCCCAGGTCAGGGGCGTGAATTTTCCCAGCAACGGCGCCGTGATGCAGAAGAAAACCAA
GGGCTGGGAGCCCAACACCGAGATGATGTACCCCGCTGACGGCGGACTGAGAGGCTACACCCACATGG
CCCTGAAGGTGGACGGCGGAGGGCACCTGAGCTGCAGCTTCGTGACCACCTACCGATCCAAGAAAACC
GTGGGCAACATCAAGATGCCCGGCATCCACGCCGTGGACCACCGGCTGGAAAGGCTGGAAGAGTCCGA
CAACGAGATGTTCGTGGTGCAGCGGGAGCACGCCGTGGCCAAGTTCGCCGGCCTGGGCGGAGGGTAA
GTCGACATAACTTCGTATAGCATACATTATACGAAGTTATGTGTCGATGGTGATGCTTGGCAATTCGGGT
CGATGGTG

Supplementary Movie 1:

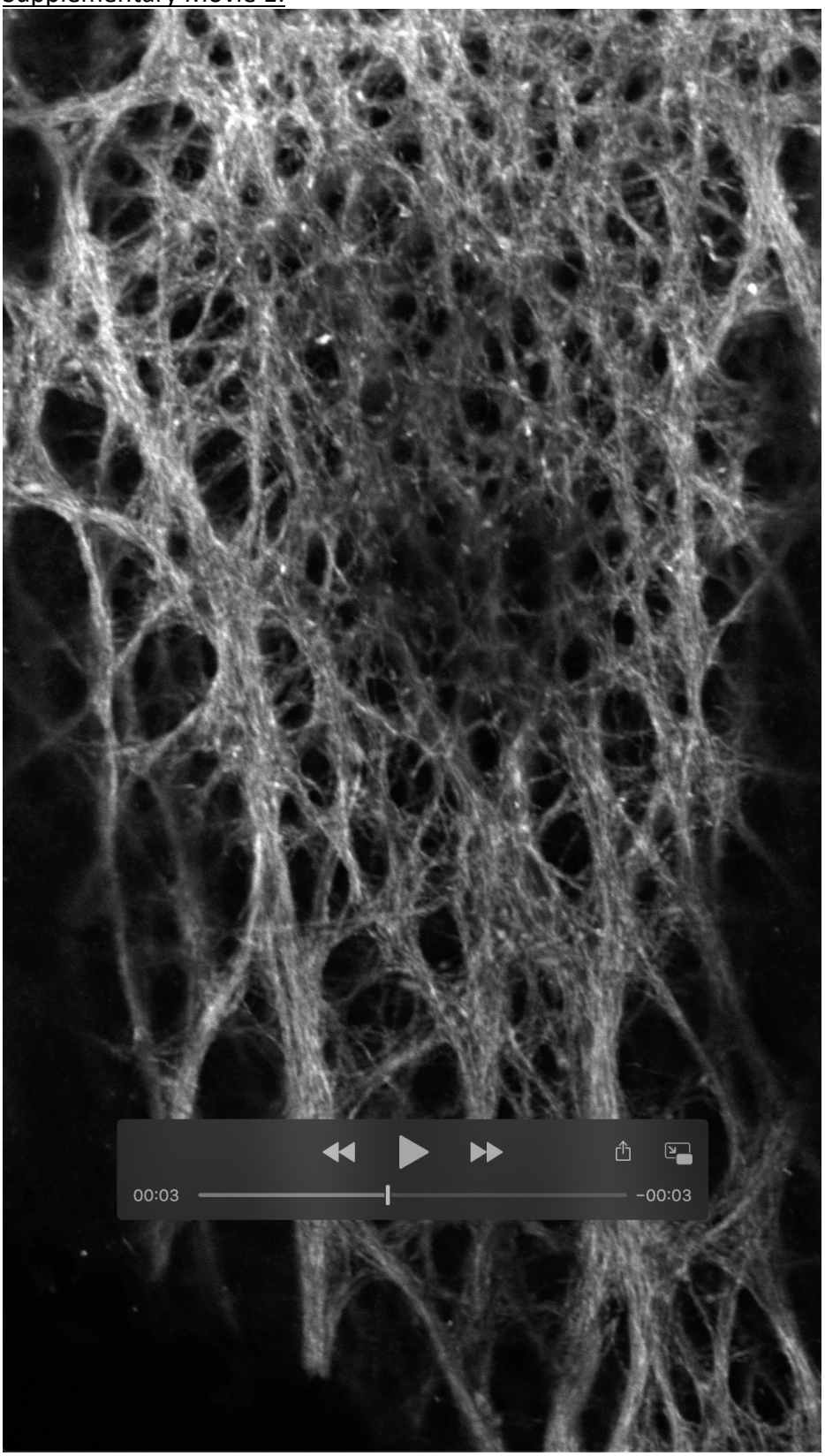
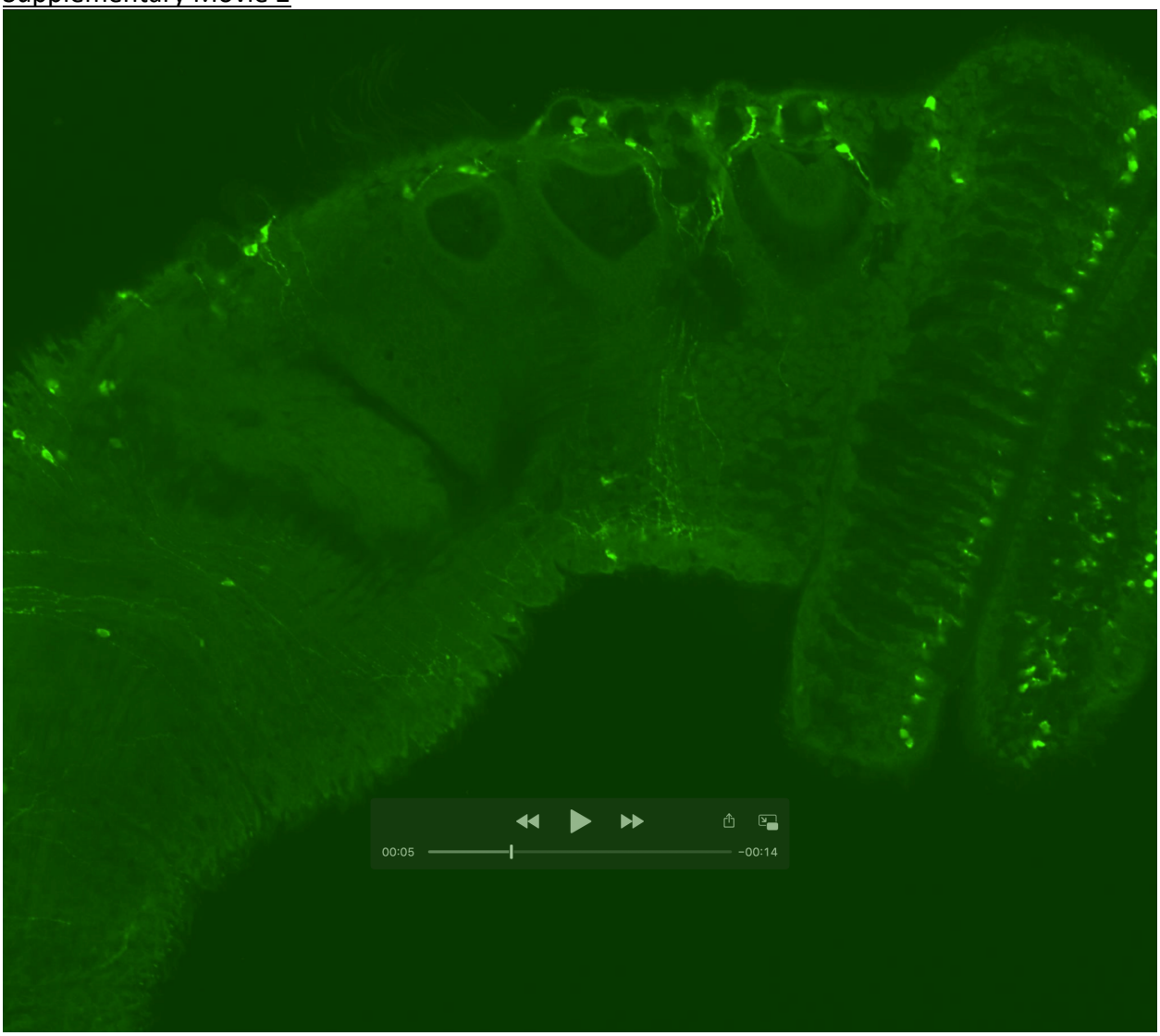
Supplementary Movie 2